antibody for 2 hr. Dilutions and sources of antibodies were as follows. The primary antibodies were: mouse monoclonal antibody against BrdU-fluorescein (Roche Diagnostics, Basel, Switzerland, 1:200), sheep polyclonal antibody against Chx10-N terminal (Exalpha Biologicals Inc., Boston, MA, 1:100), mouse monoclonal antibody against MAP2 (Sigma, St. Louis, MO, 1:200), mouse monoclonal Cy3-conjugated antibody against GFAP (Promega, 1:500), mouse polyclonal antibody against class III β tubulin (Babco, Richmond, CA, 1:500), mouse monoclonal antibody against Protein kinase C α (BD Biosciences, San Jose, CA, 1:200), mouse monoclonal antibody against vimentin (Sigma, St. Louis, MO, 1:2000) and mouse monoclonal antibody against rhodopsin kinase 1a/1b (Bio Reagents, Inc., Golden, CO, 1:200). The secondary antibodies were Alexa 488 or Alexa 594-conjugated donkey IgG against mouse IgG and Alexa 594-conjugated donkey IgG against sheep IgG. All the secondary antibodies were obtained from Molecular Probes and used at a 1:200 dilution. Negative control slides were made by omitting the primary antibody from the reaction.

For double-labelled immunocytochemistry with MAP2 and GFAP, the cells were stained with antibody against MAP-2 and visualized with a green fluorescent dye (Alexa 488) following the aforementioned protocol. Then, the samples were washed three times with PBS-T, and immunostained with a red-fluorescent dye (Cy3)-conjugated antibody against GFAP. For double-labelled immunocytochemistry with BrdU and neural markers, the cells were stained with antibody against the appropriate neural markers and visualized with red fluorescent dye (Alexa 594), and thereafter, treated with 2 M HCl for 60 min and stained with FITC-conjugated antibody against BrdU. The samples were observed under a confocal microscope (LSM510, Carl Zeiss Thornwood, NY) or an epifluorescent microscope (IX70, Olympus) as described (Yanagi et al., 2002b).

2.7. Reverse transcription-polymerase chain reaction (RT-PCR)

A reverse transcription (RT)-PCR assay was performed as described (Yanagi et al., 2002a) in order to evaluate the expression of selective markers for retinal cells in primary sphere colonies and differentiated cell cultures. Briefly, total RNA was extracted using a kit (SV total RNA extraction kit, Promega) following the manufacturer's instructions. The RNA was treated with DNase I to eliminate possible DNA contamination. An aliquot of mRNA was then converted to cDNA in a 20 μl reaction mixture using Superscript II reverse transcriptase (Gibco BRL) as recommended by the manufacturer. One microlitre of each RT reaction was then added to a standard 20 μl PCR mixture. After 9 min of preincubation at 95°C, amplification was performed for 35 cycles consisting of 30 sec of denaturing at 95°C, 30 sec of annealing at 55°C, and 30 sec of extension at 72°C. The sequences of cDNA primers and the annealing temperature are available from the authors on request. PCR products were separated on a 2% agarose gel.

3. Results

3.1. Isolation of sphere-forming progenitor cells in adult rabbits

Only the epithelial cells from the ciliary epithelium proliferated to form sphere colonies when the liquid medium was used. Iris epithelial cells, neural retinal cells, and RPE cells did not proliferate. In a typical assay, 1.0×10^6 ciliary epithelial cells were harvested per eye. Although 2–5 sphere colonies were formed per 10 000 cells in the absence of exogenous growth factors, addition of epidermal growth factor (EGF) and basic fibroblast growth factor (bFGF) facilitated the colony formation (data not shown), suggesting that only the cells from the ciliary epithelium could respond to EGF and bFGF and proliferate in vitro.

Under the current conditions using liquid medium, a substantial portion of the sphere colonies was derived from re-aggregation rather than proliferation (Kawase et al., 2004). To prevent cell-flotation and re-aggregation, we employed a culture medium that contains methylcellulose (Gritti et al., 1996; Kawase et al., 2004), and investigated whether these sphere colonies form from proliferation rather than the re-aggregation of previously dissociated cells. First, to directly address whether the cells actually proliferated, the cell culture was carefully monitored with an inverted microscope. Under these conditions, cell proliferation was accompanied by little cell flotation (Fig. 2A–F). To examine whether the cells were indeed dissociated, cell nuclei were stained with Hoechst dye immediately after plating and percentages of single cells, doublets and triplets were calculated. As expected, more than 90% of the cells were single cells (Table 1). Next, to investigate whether cell aggregation occurs during culture, we examined the cells for up to 48 hr, before most cells show a robust proliferation. The proportion of single cells was 90% (Table 1), similar to the result obtained immediately after plating, suggesting little cell aggregation. Additionally, we mixed CFDA-labelled and un-labelled cells and found that cell aggregation did not occur 24 hr later (Fig. 2G). Together, these results suggest that most sphere colonies are derived from proliferation, but not re-aggregation when a methylcellulose gel matrix is used.

It was demonstrated that the cells actually divided to form sphere colonies upon incubation with BrdU for 24 hr before fixation (Fig. 3B). The spheres expressed Chx10, a marker of retinal progenitor cells (Fig. 3C). They were not stained for mature neuronal cell markers including the pan-neuronal marker, microtubule-associated protein 2 (MAP2), and the astrocytic marker, glial fibrillary acidic protein (GFAP) (data not shown).

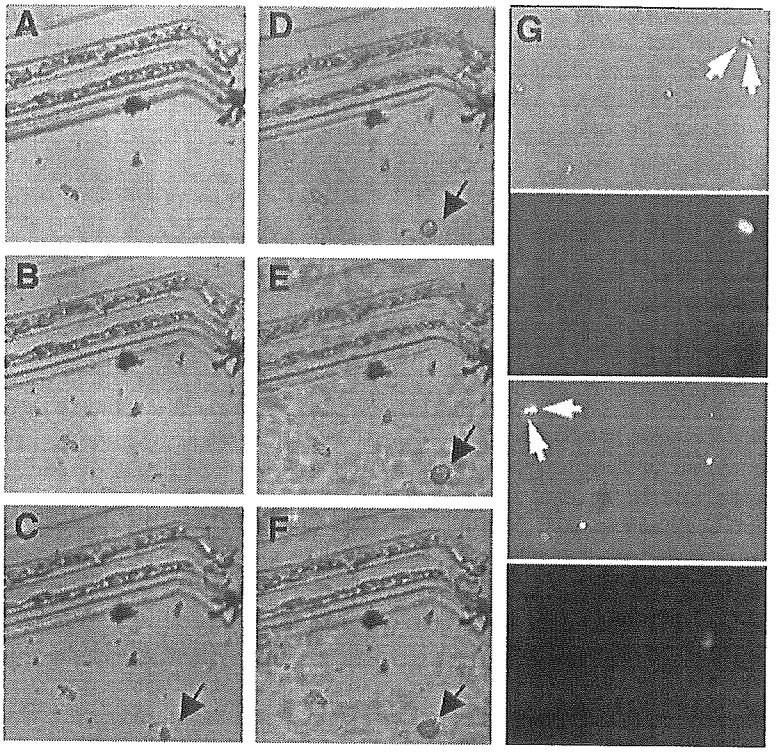

Fig. 2. Time lapse observation of cell culture. (A–F) Time lapse observation of the cell culture in a methylcellulose gel matrix. A proportion of the culture was imaged for 7 days at intervals of 24–48 hr, beginning immediately after plating. Images were obtained 24 hr (A), 48 hr (B), 3 days (C), 4 days (D), 6 days (E) and 8 days (F) after plating. The bottom of the plate was scratched with a Pasteur pipette to identify the location. Note that the sphere colonies (arrows in C–F) become visible three days after plating (C) and that little cell-flotation is observed. (G) A portion of the cells were labelled with CFDA, mixed with unlabelled cells and cultured in 24-well culture dishes. The culture was observed with an epifluorescent microscope 24 hr after plating to investigate the presence of the mixture of cells. The first and third panels show the phase contrast micrographs of the cell culture. The second and last panels show fluorescent micrographs of the same field in the first and third panels, respectively. Note that the cell-doublets (arrows in the first and third panels) consist of two CFDA-positive (second panel) or two CFDA-negative (last panel) cells. More than 100 doublets were examined. No cell-doublets consisted of a mixture of CFDA-positive and negative cells.

3.2. Passagability of the spheres derived from ciliary epithelium

Next, we examined whether the cells dissociated from the primary spheres generated in the methylcellulose gel matrix could proliferate to generate secondary sphere colonies. Secondary sphere formation occurred in the methylcellulose gel matrix (Table 2), confirming that some of the cells had the potential to self-renew. When single primary sphere colonies were dissociated into single cells and the progeny plated into individual wells, 13.6% of the primary sphere colonies gave rise to secondary sphere colonies. The fact that small spheres are difficult to passage may be the reason that some sphere colonies did not generate secondary colonies after passage, so we collected five primary sphere colonies in a microtube and dissociated them into single cells and plated all the cells from the five sphere colonies into a single well. Even with this method, we found that 44% of the wells contained secondary sphere colonies.

Tertiary spheres also formed under the same conditions (Table 2), suggesting again that some of these cells could self-renew. However, after 2 months in vitro, the cells became senescent and could not be passaged. The primary, secondary, and tertiary sphere colonies were similar in diameter (Table 2).

To circumvent the confounding effect of the methylcellulose gel matrix, we also tested the replating efficiency with the liquid medium without methylcellulose. Although the diameter of the sphere colonies was greater in the absence of methylcellulose, the numbers of secondary and tertiary sphere colonies were reduced compared to those generated in the medium containing methylcellulose (Table 2).

Table 1
Percentage of single cells, doublets and triplets immediately and 48 hr after culturing in methylcellulose gel matrix

	Single cells	Doublets	Triplets
Immediately after plating	90.7±2.6	6.4±1.9	2.9±0.9
48 hr after plating	89.8±2.8	6.8±1.9	3.4±1.1

To investigate the cells dissociated into single cells, the cell nuclei were counterstained with Hoechst dye and the single cells, doublets, and triplets were enumerated immediately and 48 hr after plating ($n=6$).

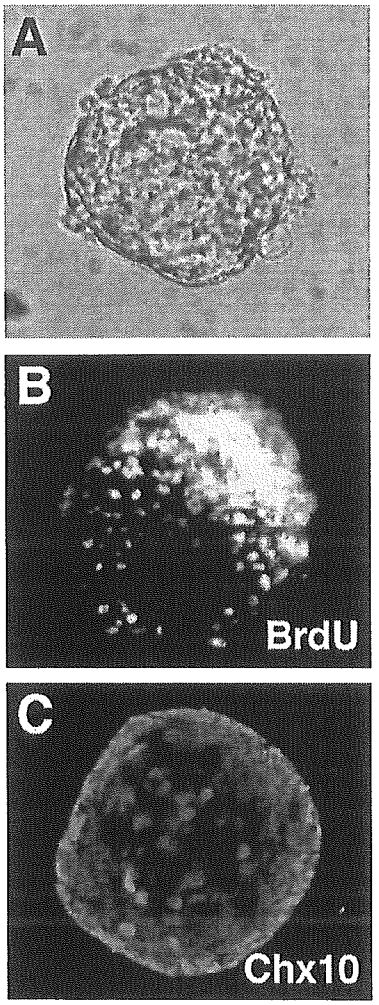

Fig. 3. Immunostaining of sphere colonies. Sphere colonies generated in a methylcellulose gel matrix (A) incorporated BrdU when exposed to BrdU 24 hr before fixation (B) and expressed Chx10 (C), a marker for retinal progenitor cells. The sphere colonies did not express mature neural markers such as MAP-2 and GFAP (data not shown).

Similar to the results obtained in the absence of methylcellulose; the cells became senescent after 2 months in culture.

3.3. Potential to differentiate of progenitor cells derived from ciliary epithelium

To test whether the cells from primary spheres generated in the methylcellulose gel matrix can differentiate into retinal neurons expressing selective markers for retinal cells, cells dissociated from primary spheres were cultured in bulk in DMEM/F12 containing 1% FBS or bFGF for 14 days and immunolabelled with a photoreceptor marker, GRK 1a/b, a Müller cell marker, vimentin and a bipolar cell marker, protein kinase C α (PKCα). It was demonstrated that the sphere colonies were labelled with these markers (Fig. 4A–C). Cells from secondary spheres were also positively immunolabelled with GRK 1a/b, vimentin and PKCα after their differentiation (data not shown).

To further confirm the differentiation potency of the sphere colonies, we analysed the expression of genes which are expressed in the neural retina and whose cDNA sequences are currently available in rabbits. We confirmed that the neural retina expresses βIII tubulin, vimentin and calbindin at the mRNA level. mRNA of βIII tubulin and vimentin were also detected in the ciliary epithelium. We found that the differentiated progeny expressed vimentin, calbindin, and βIII tubulin, whereas none of these markers were expressed at detectable levels in the sphere colonies (Fig. 4D), confirming the results of the immunocytochemical analysis.

Next, we investigated whether the cells were immunolabelled with pan-neuronal and astrocytic markers. Fourteen days after each sphere colony was plated onto individual wells of poly-L-lysine/laminin-coated dishes in the presence of 1% fetal bovine serum (FBS), the cells that had attached to the plate and migrated away from the sphere colonies expressed an immature neuronal marker, βIII tubulin (TuJ1), mature neuronal markers, MAP2, and a glial cell marker, GFAP (Fig. 5A–C). When BrdU was added to the medium immediately after the differentiation, cells that incorporated BrdU expressed βIII tubulin, MAP-2 and GFAP (Fig. 5A–C), suggesting that they actually divided. Similarly, when secondary spheres were allowed to differentiate under the same conditions, the cells also expressed MAP2 and GFAP (data not shown). When single primary sphere colonies were examined with double-labelled immunocytochemistry for MAP-2 and GFAP (Fig. 5D), 23% of the progeny of individual spheres were double-labelled with MAP-2 and GFAP antibodies, and 5.6 and 68% exclusively with the MAP-2 and GFAP antibodies, respectively.

Table 2
Number and diameter of spheres from the rabbit ciliary epithelium

Methylcellulose gel matrix	Primary	Secondary	Tertiary
n	4	3	2
No. of sphere colonies (/10 000 cells)	10.6±2.2	98.5±22.6	81
Diameter of sphere colonies (μm)	74.0±8.3	81.0±1.4	81
Medium without methylcellulose	**Primary**	**Secondary**	**Tertiary**
n	6	6	1
No. of sphere colonies (/10 000 cells)	10.4±1.7	40.5±4.3	19
Diameter of sphere colonies (μm)	278±61	116±18.9	98

Cultures were observed with an inverted microscope and images were analysed with an NIH imaging program. Data are shown as the mean±S.E.M..

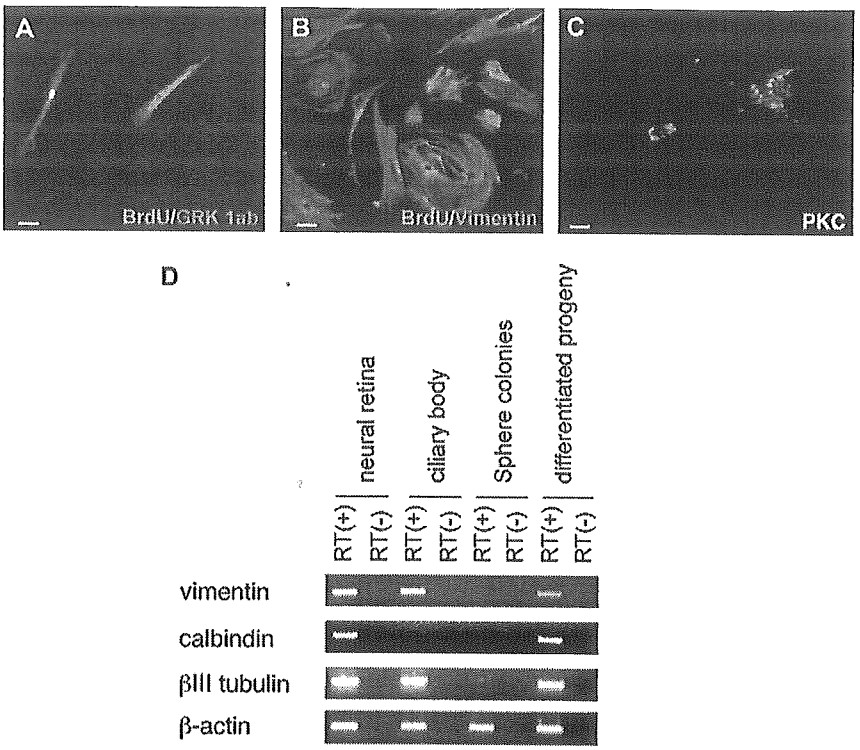

Fig. 4. Expression of retinal selective antigens in cells differentiated from sphere colonies. Cells dissociated from primary spheres were plated onto poly-L-lysine/lamine-coated dishes in the presence of 1% FBS, exposed to BrdU immediately (A and B), and cultured for 14 days. In (C), 24 hr after plating, the cells were washed with medium and cultured in the absence of FBS and in the presence of bFGF. Differentiated progeny that formed the sphere colonies and incorporated BrdU (A and B, green) were stained with GRK 1a/b (A), vimentin (B) (red), and PKCα (C, green). Cell nuclei were stained with Hoechst 33342 in (C). (D) In sphere colonies and their differentiated progeny RT-PCR analysis was performed to investigate the expression of genes which are expressed in the mature neural retina and whose cDNA sequences are available in rabbits, i.e. βIII tubulin, vimentin and calbindin. Note that all the genes are expressed in the differentiated progeny, whereas no expression was detected in the sphere colonies. Scale bars, (A, B) 20 μm, (C) 30 μm.

4. Discussion

Previous investigators demonstrated that the far peripheral retinal regions in adult vertebrates contain retinal progenitor cells (Ahmad et al., 2000; Tropepe et al., 2000). Well consistent with studies using mice (Tropepe et al., 2000) and rats (Ahmad et al., 2000), our results indicate that the ciliary epithelium of adult rabbits contains retinal progenitor cells; a progenitor enriched population was obtained by neurosphere assay and the differentiated progeny of the sphere colonies, but no sphere colonies themselves, expressed not only neuronal and glial markers, but also selective markers for retinal cells. This is the first report of retinal progenitor cells isolated from adult rabbit eyes.

We employed culture conditions under which the cells proliferate without re-aggregating. Of note, it was previously demonstrated that multipotential neural stem-like cells from the adult forebrain can proliferate clonogenically using a methylcellulose gel matrix similar to that used in the present study (Gritti et al., 1999). However, to date, retinal progenitors from the ciliary epithelium have not been studied clonogenically. Herein, it was demonstrated that the sphere colonies from adult ciliary epithelium contain many distinct progenitor subtypes; approximately 80% of the primary sphere colonies were unipotential neuronal or glial progenitors that generate either MAP2-positive neurons or GFAP-positive glial cells exclusively and approximately 20% are bipotential progenitors that can give rise to both neurons and glia. Because our culture started with 90% single cells and approximately 10% doublets and triplets, it is reasonable to conclude the actual percentage of bipotential progenitor cells is less than 20%. Moreover, it was estimated that only a minor portion of the primary sphere colonies gave rise to secondary sphere colonies, whereas the rest did not proliferate to generate daughter colonies. Previous studies have demonstrated that unipotential progenitor cells generally have limited potential to proliferate and do not give rise to secondary sphere colonies, whereas multipotential progenitors show a robust proliferation and generate secondary sphere colonies when the neurosphere assay is used to enrich a population with neural progenitor cells (Chiasson et al., 1999; Seaberg and van der Kooy, 2002). Thus, it is likely that progenitor cells from bipotential sphere colonies gave rise to secondary sphere colonies and those from unipotential sphere colonies did not. The most rational interpretation for the heterogeneity of the sphere colonies would be that the ciliary epithelium

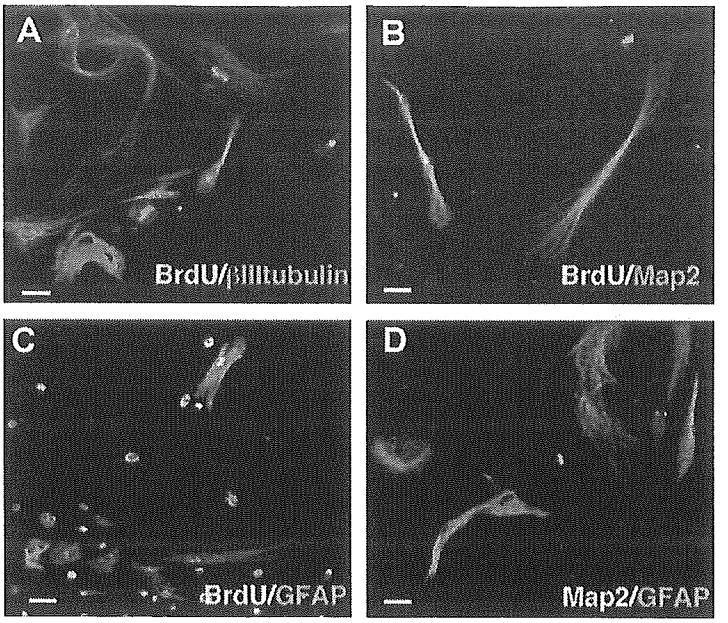

Fig. 5. Immunostaining of cells differentiated from spheres. (A–D) Each sphere colony was plated onto individual well of poly-L-lysine/laminin-coated dishes in the presence of 1% FBS and cultured for 14 days. (A–C) Cells were exposed to BrdU immediately after they were plated onto poly-L-lysine/laminin-coated dishes. Sphere-derived cells that incorporated BrdU (green) expressed the immature neuronal marker β III tubulin (A), mature neuronal marker MAP2 (B), and the astrocytic cell marker GFAP (C) (red). (D) A representative result of double-labelled immunostaining with MAP-2 and GFAP antibodies is shown. Note that both MAP-2-positive (green) and GFAP-positive (red) cells are present in the progeny derived from a single sphere. The percentage of sphere colonies that expressed with both MAP-2 and GFAP were 23%. No cells were double-labelled with both antibodies. The cell nuclei were counter stained with Hoechst 33342. Scale bars, (A, B, C) 20 μm, (D) 15 μm.

contains subpopulations of progenitor cells with various phenotypes and most of the progenitor cells are glial progenitor cells. Thus, our results indicate that the ciliary epithelium of adult rabbits contains both (at least) bipotential retinal progenitor (or stem) cells and unipotential fate-restricted progenitor cells, similar to lower vertebrates.

Our results demonstrate that bFGF and EGF promote cell division among retinal progenitors in rabbits. Although a small number of sphere colonies were generated in the absence of exogenous growth factors, the colony formation was much facilitated by the additions of bFGF and EGF. Thus, adult retinal progenitor cells in the rabbit are partially dependent on exogenous growth factors, which is in contrast to adult retinal stem cells in mice (Tropepe et al., 2000). However, even in the presence of these growth factors, our results also demonstrate that only a relatively small population of the propagated cells in the sphere can proliferate after passage and that the cells become senescent after the fourth or fifth passage (2 months) in vitro. The diameter of the sphere colonies generated in the absence of methylcellulose was greater. However, even when the cells were cultured in the absence of methylcellulose, the number of the sphere colonies was reduced compared to those generated in methylcellulose gel matrix and the cells became senescent in 2 months. Addition of known retinal mitogens such as BDNF, CNTF, TGF-α, and acidic FGF did not facilitate sphere colony formation (data not shown), suggesting that other factors are required to promote a proliferation maintaining progenitor cell state in vitro and/or that these cells intrinsically possess only a limited proliferative capability.

In rabbits, approximately 10 sphere colonies are generated from 10 000 ciliary epithelial cells. Thus, the number of sphere-initiating cells in the ciliary epithelium is smaller than that in mice, in which approximately 0.2% of ciliary epithelial cells can give rise to sphere colonies (Tropepe et al., 2000). The diameter of the sphere colonies is also smaller in rabbits (81–271 μm) than in mice (~300 μm) (Tropepe et al., 2000). Moreover, as mentioned above, only a minor portion of the primary sphere colonies could generate secondary sphere colonies in rabbits. This is in contrast to the situation in mice in which individual primary sphere colonies can be subcultured to give rise to secondary sphere colonies. It should be noted that the differentiated progeny of the sphere colonies in rabbits expressed a bipolar cell marker, photoreceptor cell marker and a Müller cell marker, similar to these in mice (Tropepe et al., 2000) and rats (Ahmad et al., 2000). We also found that the differentiated progeny in rabbits expressed calbindin, a marker expressed in horizontal cells. Thus, the properties of growth and differentiation of isolated retinal progenitor cells in rabbits are different from those in mice (Tropepe et al., 2000) and rats (Ahmad et al., 2000) in some respects, although there are certain similarities.

A recent study demonstrated that retinal progenitor cells isolated from the ciliary epithelium can be incorporated into

retina and express some retinal cell markers in mice or rats (Chacko et al., 2003). To clarify whether the adult retinal progenitor cell can be used for cell-based transplantation therapy in humans, laboratory studies, including transplantation experiments using animals as a disease model, are required. The rabbit is one of the suitable species for transplantation experiments, because its relatively large eyes enable one to design surgical procedures that can be used in humans (Wasselius and Ghosh, 2001). Additionally, several studies have reported that drug-induced retinal damage in rabbits can be used as a model for human diseases (Grignolo et al., 1966; Orzalesi et al., 1967). We believe that rabbits are one of the best animal models for such transplantation experiments, because of their relatively large eyes, which allow one to perform reproducible and reliable surgery. Cultured spheres from the rabbit ciliary epithelium, however, are not homogenous and most of the spheres contain glial progenitors.

References

Ahmad, I., Tang, L., Pham, H., 2000. Identification of neural progenitors in the adult mammalian eye. Biochem. Biophys. Res. Commun. 270, 517–521.

Cepko, C.L., Austin, C.P., Yang, X., Alexiades, M., Ezzeddine, D., 1996. Cell fate determination in the vertebrate retina. Proc. Natl Acad. Sci. USA 93, 589–595.

Chacko, D.M., Das, A.V., Zhao, X., James, J., Bhattacharya, S., Ahmad, I., 2003. Transplantation of ocular stem cells: the role of injury in incorporation and differentiation of grafted cells in the retina. Vision Res. 43, 937–946.

Chiasson, B.J., Tropepe, V., Morshead, C.M., van der Kooy, D., 1999. Adult mammalian forebrain ependymal and subependymal cells demonstrate proliferative potential, but only subependymal cells have neural stem cell characteristics. J. Neurosci. 19, 4462–4471.

Grignolo, A., Orzalesi, N., Calabria, G.A., 1966. Studies on the fine structure and the rhodopsin cycle of the rabbit retina in experimental degeneration induced by sodium iodate. Exp. Eye Res. 5, 86–97.

Gritti, A., Parati, E.A., Cova, L., Frolichsthal, P., Galli, R., Wanke, E., Faravelli, L., Morassutti, D.J., Roisen, F., Nickel, D.D., Vescovi, A.L., 1996. Multipotential stem cells from the adult mouse brain proliferate and self-renew in response to basic fibroblast growth factor. J. Neurosci. 16, 1091–1100.

Gritti, A., Frolichsthal-Schoeller, P., Galli, R., Parati, E.A., Cova, L., Pagano, S.F., Bjornson, C.R., Vescovi, A.L., 1999. Epidermal and fibroblast growth factors behave as mitogenic regulators for a single multipotent stem cell-like population from the subventricular region of the adult mouse forebrain. J. Neurosci. 19, 3287–3297.

Harris, W.A., 1997. Cellular diversification in the vertebrate retina. Curr. Opin. Genet. Dev. 7, 651–658.

Jumblatt, M.M., Raphael, B., Jumblatt, J.E., 1991. A simple method for the isolation of ciliary epithelium. Exp. Eye Res. 52, 229–232.

Kawase, Y., Yanagi, Y., Takato, T., Fujimoto, M., Okochi, H., 2004. Characterization of multipotent adult stem cells from the skin: transforming growth factor-beta (TGF-beta) facilitates cell growth. Exp. Cell Res. 295, 194–203.

Moshiri, A., Reh, T.A., 2004. Persistent progenitors at the retinal margin of ptc ± mice. J. Neurosci. 24, 229–237.

Orzalesi, N., Grignolo, A., Calabria, G.A., Castellazzo, R., 1967. A study on the fine structure and the rhodopsin cycle of the rabbit retina in experimental degeneration induced by diaminodiphenoxypentane. Exp. Eye Res. 6, 376–382.

Perron, M., Harris, W.A., 2000. Retinal stem cells in vertebrates. Bioessays 22, 685–688.

Reh, T.A., Levine, E.M., 1998. Multipotential stem cells and progenitors in the vertebrate retina. J. Neurobiol. 36, 206–220.

Reynolds, B.A., Tetzlaff, W., Weiss, S., 1992. A multipotent EGF-responsive striatal embryonic progenitor cell produces neurons and astrocytes. J. Neurosci. 12, 4565–4574.

Seaberg, R.M., van der Kooy, D., 2002. Adult rodent neurogenic regions: the ventricular subependyma contains neural stem cells, but the dentate gyrus contains restricted progenitors. J. Neurosci. 22, 1784–1793.

Troncoso, M., 1942. Microanatomy of the eye with slitlamp microscope. II. Comparative anatomy of the ciliary body, zonula and related structures in mammalia. Am. J. Ophthalmol. 25, 1–31.

Tropepe, V., Coles, B.L., Chiasson, B.J., Horsford, D.J., Elia, A.J., McInnes, R.R., van der Kooy, D., 2000. Retinal stem cells in the adult mammalian eye. Science 287, 2032–2036.

Wasselius, J., Ghosh, F., 2001. Adult rabbit retinal transplants. Invest. Ophthalmol. Vis. Sci. 42, 2632–2638.

Wolosin, J.M., Chen, M., Gordon, R.E., Stegman, Z., Butler, G.A., 1993. Separation of the rabbit ciliary body epithelial layers in viable form: identification of differences in bicarbonate transport. Exp. Eye Res. 56, 401–409.

Yanagi, Y., Takezawa, S., Kato, S., 2002a. Distinct functions of photoreceptor cell-specific nuclear receptor, thyroid hormone receptor beta2 and CRX in cone photoreceptor development. Invest. Ophthalmol. Vis. Sci. 43, 3489–3494.

Yanagi, Y., Tamaki, Y., Obata, R., Muranaka, K., Homma, N., Matsuoka, H., Mano, H., 2002b. Subconjunctival administration of bucillamine suppresses choroidal neovascularization in rat. Invest. Ophthalmol. Vis. Sci. 43, 3495–3499.

Zhao, X., Huang, J., Khani, S.C., Palczewski, K., 1998. Molecular forms of human rhodopsin kinase (GRK1). J. Biol. Chem. 273, 5124–5131.

Available online at www.sciencedirect.com
SCIENCE DIRECT®
Experimental Eye Research 82 (2006) 471–478
EXPERIMENTAL EYE RESEARCH
www.elsevier.com/locate/yexer

Properties of growth and molecular profiles of rat progenitor cells from ciliary epithelium

Yasuo Yanagi[a,b,*], Yuji Inoue[a,b], Yoko Kawase[a], Saiko Uchida[b], Yasuhiro Tamaki[b], Makoto Araie[b], Hitoshi Okochi[a]

[a]*Department of Regenerative Medicine, Research Institute, International Medical Center of Japan, 1-21-1 Toyama, Shinjuku-ku, Tokyo 162-8655, Japan*
[b]*Department of Ophthalmology, University of Tokyo School of Medicine, 7-3-1 Hongo, Bunkyo-ku, Tokyo 113-8655, Japan*

Received 17 April 2005; accepted in revised form 8 August 2005
Available online 29 September 2005

Abstract

Recent studies have demonstrated that multipotent retinal stem or progenitor cells can be isolated from the ciliary epithelium (CE) of the eye using a neurosphere culture. In this study, we investigated the properties of growth and differentiation, and molecular profiles of rat adult ciliary epithelium (CE)-derived retinal progenitors and forebrain (FB) derived neurospheres. Under clonogenic culture conditions, we found that the CE-derived neurospheres contained fewer undifferentiated cells compared with the FB-derived neurospheres, and that CE-derived neurospheres initially expressed the set of Notch pathway molecules genes including Notch 1 and Delta 1, HES-1 and HES-5, but partially lose their expression after passaging. Furthermore, we found that the CE-derived neurospheres did not express several markers for in vivo embryonic retinal progenitors. Additionally, when the eye was divided into four subregions along its dorsoventral and nasotemporal axes and progenitor cells were obtained from the subregions, the progenitor cells did not express the subregion specific transcription factors, suggesting that subregional specificity is not maintained in vitro. Together, our results demonstrate that CE-derived progenitor cells may have intrinsic limitations in the production of cell types.

Keywords: retinal cell differentiation; Retinal cell lineages; Ciliary epithelium; Retinal cell culture

1. Introduction

Recent studies have demonstrated that multipotent retinal stem or progenitor cells can be isolated from the ciliary epithelium (CE) using a neurosphere culture (Ahmad et al., 2000; Tropepe et al., 2000). A study using mice (Tropepe et al., 2000) demonstrated that one in 500 CE cells give rise to a neurosphere consisting of ~12 000 cells with retinal neural properties and that an individual neurosphere contains cells which can generate six to eight daughter neurosphere colonies. This may imply that a smaller number of the daughter neurosphere colonies is generated from individual CE-derived neurospheres compared with the neurospheres from other regions including embryonic forebrain (FB) (Reynolds et al., 1992; Reynolds and Weiss, 1996) and adult subventricular zone (Morshead et al., 1994), from which approximately 20% of the cells within a neurosphere can generate daughter colonies. However, the growth properties of the rat CE-derived retinal progenitor cells have not been extensively described (Ahmad et al., 2000; Tropepe et al., 2000).

Much less is known about the molecules expressed to define regional specificity of CE-derived retinal progenitor cells. Previous studies have shown that CE-derived neurosphere colonies in mice and rats express one of the retinal specific transcription factors, Chx10 (Ahmad et al., 2000; Tropepe et al., 2000). It is well-known that several other transcription factors are essential for embryonic or postnatal retinal progenitors to generate complete sets of mature retinal cell types (Cepko et al., 1996). For example, transcription factors including homeodomain transcription factors such as Pax2, Pax6, Six3 and Rx (Dressler et al., 1990; Furukawa et al., 1997; Gruss and Walther, 1992; Mathers et al., 1997; Nornes et al., 1990; Oliver et al., 1995)

* Corresponding author. Tel.: +81 3 5800 8660; fax: +81 3 3817 0798.
E-mail address: yanagi-tky@umin.ac.jp (Y. Yanagi).

0014-4835/$ - see front matter © 2005 Elsevier Ltd. All rights reserved.
doi:10.1016/j.exer.2005.08.005

define specification of the retinal primordial. The embryonic or postnatal retinal progenitor cells also express region-specific transcriptional factors such as Chx10, RORβ and Foxn4 (Burmeister et al., 1996; Chow et al., 1998; Gouge et al., 2001). Notably, the retina itself is also patterned along dorsoventral and nasotemporal axes. In the dorso-ventral axis of the retina, graded expressions of homeobox gene Tbx5 determines dorsal identity, whereas another class of homeobox gene, Vax2, defines the ventral identity (Barbieri et al., 2002; Schulte et al., 1999). EphAs are expressed in a low to high naso-temporal gradient in retina, whereas ephrins are expressed in a high to low naso-temporal gradient (Pittman and Chien, 2002). Previous studies have demonstrated that isolated neural stem cells from spinal cord (Yamamoto et al., 2001) or different regions of brain (Hitoshi et al., 2002) express different regional markers after culturing. It is also important to examine which regional specific transciption factors are also expressed in the CE-derived retinal progenitors to estimate their differentiation potential.

In the current study, we obtained progenitor cells from four subdivision of the rat CE and the embryonic forebrain (FB) (Reynolds et al., 1992; Reynolds and Weiss, 1996), and compared their growth properties and expression pattern of region specific transcription factors. Concomitantly, we examined the expression of stem cell factors defining the 'stemness'(Ramalho-Santos et al., 2002) such as Notch signaling pathway molecules (Bao and Cepko, 1997; Tomita et al., 1996).

2. Materials and methods

2.1. Animals

Wister rats (6–8 weeks old) were obtained from Saitama Experimental Animal Supply Co. Ltd (Saitama, Japan). All experiments were conducted in accordance with the Animal Care and Use Committee and the Association for Research in Vision and Ophthalmology Statement for the Use of Animals in Ophthalmic and Vision Research.

2.2. Isolation of progenitor cells from ciliary epithelium

Ciliary epithelium (CE)-derived progenitor cell was isolated as described elsewhere (Ahmad et al., 2000; Tropepe et al., 2000). Briefly, the ciliary epithelium was dissected and digested with 0.25% trypsin for 10 min. To divide the eye into four subregions, a small incision made by scissors to mark the dorsal side of the eye before enucleation, and the eye was carefully removed and divided into four subdomains along its dorso-ventral and naso-temporal axes. Then, the ciliary epithelial cells were isolated from each region. The tissue was then mechanically dissociated in DMEM and F-12 medium (Invitrogen, Rockville, MD), washed once with soy bean trypsin inhibitor, and the cell suspension was poured through a 40 μM cell strainer (Beckton Dickinson Labwere, Franklin Lakes, NJ). Primary culture was performed as previously described (Reynolds et al., 1992) with some modifications. We used medium containing methylcellulose to prevent cell re-aggregation similar to our previous studies (Inoue et al., 2005; Kawase et al., 2004), which was established by previous investigators to isolate clonogenic neural stem cells (Gritti et al., 1999; Gritti et al., 1996). In brief, cell culture was performed using methylcellulose gel matrix (Wako, Osaka, Japan) dissolved in a DMEM and F-12 medium. The cells were seeded at a density of 10 viable cells/μl in a DMEM and F-12 medium supplemented with the B-27 culture supplement (Invitrogen), 20 ng/ml bovine basic fibroblast growth factor (bFGF) (Peprotech EC LTD, London, U.K), 20 ng/ml mouse epidermal growth factor (EGF) (Antigenix America Inc., NY, U.S.A.), 2 g/ml heparin (Sigma, St. Louis, MO)

2.3. Isolation of stem cells from the embryonic forebrain

The striatal primordia was dissected from the embryonic day 14 (E14) embryonic forebrain as described previously (Reynolds et al., 1992). The tissue from each embryo was transferred to a DMEM and F-12 medium and mechanically triturated into single cell. The cells were cultured under the same conditions, i.e. they were seeded in methylcellulose gel matrix dissolved in a DMEM and F-12 medium supplemented with the B-27 culture supplement, 20 ng/ml bFGF, 20 ng/ml EGF and 2 g/ml heparin at a density of 10 viable cells/μl.

2.4. Cell passaging

To passage the neurospheres, sphere colonies obtained after 7 days in culture were collected, dissociated into single cells by trypsinization, plated into 24 well dishes at a cell density of 10 cells/μl in 24 well dish plates and cultured for further 7 days under the same condition. Cells were passaged every 7 days thereafter.

To measure the diameter of the neurosphere colonies, the cultures were observed with an inverted microscope (Olympus BX-51, Tokyo, Japan) and the images were imported into a Macintosh computer with an aid of CCD camera (Olympus DP50) and were analyzed by NIH image program developed at National Institute of Health and available on the Internet at http://rsb.info.nih.gov/nih-image/.

2.5. Differentiation of sphere-derived cells

For differentiation, spheres or singly dissociated cells from the neurospheres were allowed to attach to poly-D-lysine/laminin coated 24 well dishes for 7 days in the presence of 1% fetal bovine serum (FBS) and bFGF at a final concentration of 10 ng/ml.

2.6. Immunocytochemistry

Neurospheres or cells were washed with PBS, and fixed in absolute methanol for 30 min at 4 °C and blocked in PBS containing 1% skim milk for 10 min. The samples were then incubated with the primary antibodies at room temperature for two hours, rinsed twice with the blocking buffer, and incubated with the secondary antibody for two hours. Dilutions and sources of antibodies were as follows. The primary antibodies were: mouse monoclonal antibody against neurofilament-M (NF-M; Sigma 1:200), rabbit polyclonal antibody against GFAP (Dako, Glostrup, Denmark, 1:500) and mouse monoclonal antibody against O4. The secondary antibodies were Alexa 488 conjugated donkey IgG against mouse IgG and Alexa 488 conjugated donkey IgG against rabbit IgG. All the secondary antibodies were obtained from Molecular Probes at Eugene in OR and used at a 1:200 dilution. Negative control slides were made by omitting the primary antibody from the reaction. The samples were observed under a confocal microscope LSM510 (Carl Zeiss Thornwood, NY) or an epifluorescent microscope (IX70, Olympus).

2.7. RNA isolation and reverse-transcriptase polymerase chain reaction (RT-PCR)

Total RNA was extracted using a kit (SV total RNA extraction kit, Promega) following the manufacturer's instructions. The RNA was treated with DNase I to eliminate possible DNA contamination. Two microgram of mRNA was then converted to cDNA in a 20 μl reaction mixture using Superscript II reverse transcriptase (Gibco BRL, Rockville, MD USA) as recommended by the manufacturer. One micro litre of each RT reaction was then added to a standard 50 μl PCR mixture. After 5 min of preincubation at 95 °C, amplification was performed for 30 cycles consisting of 1 min of denaturing at 95 °C, 1 min of annealing at appropriate temperature, and 1 min extension at 72 °C. The sequences of cDNA primers and annealing temperature are available at request from authors. As dorsoventral markers, Vax2 and Tbx5 were employed. However, our preliminary experiments failed to demonstrate any Eph and ephrins to be expressed in a graded fashion along its nasotemporal axis in rats, and nasotemporal retinal cell markers were unavailable. PCR products were separated on 2% agarose gel. The sequences of these fragments were completely identical to transcripts. Preliminary experiments established that under this condition of PCR, the amounts of each transcript were semiquantitative.

3. Results

3.1. Potential of differentiation and proliferation of the rat ciliary epithelium derived-progenitor cells

First, we compared the potential of differentiation of progenitor cells from the adult ciliary epithelium and embryonic forebrain. Embryonic forebrain contains highly proliferative stem cells that have been extensively studied and well characterized (Reynolds et al., 1992; Reynolds and Weiss, 1996). Tissues from the adult ciliary epithelium and embryonic forebrain were subjected to primary cultures, and proliferative progenitors were enriched as neurospheres in the presence of FGF2 and EGF as described (Reynolds et al., 1992; Reynolds and Weiss, 1996; Tropepe et al., 2000). These neurosphere-forming cells could be maintained by repeated passages for 6 weeks, and nearly all the neurosphere-forming cells from both groups expressed Nestin, an intermediate filament expressed in, but not specific for, undifferentiated neural precursors, similar to the previous studies (data not shown) (Reynolds et al., 1992; Reynolds and Weiss, 1996; Tropepe et al., 2000). Differentiated progenies from the CE-derived neurospheres expressed a neuronal marker, NF-M, and an astrocytic marker, GFAP (Fig. 1A and B). Expression of a photoreceptor-cell specific homeobox gene, CRX, was also detected by RT-PCR (Fig. 1C). In contrast, the progeny from the embryonic forebrain derived neurospheres expressed NF-M, GFAP and O4 as demonstrated by immunocytochemistry, but did not express detectable levels of CRX by RT-PCR (Fig. 1C–F), consistent with the previous studies (Tropepe et al., 2000). Progenitors in the adult ciliary epithelium did not generate neurons expressing Thy-1 and HPC-1, specific molecular markers for retinal ganglion cells and amacrine cells, respectively, and O4-positive oligodendrocyte. The morphology of the neuronal cells from the ciliary epithelium and forebrain was different. Most NF-M positive cells from the ciliary epithelium are bipolar; in contrast, NF-M positive cells from the embryonic forebrain have multiple cell processes (compare Fig. 1A and D). Thus, the potential of differentiation was different between progenitors isolated from ciliary epithelium and embryonic forebrain.

Next, we compared the proliferative potential of progenitor cells from the adult ciliary epithelium and embryonic forebrain. The number of secondary and tertiary neurosphere colonies from the adult ciliary epithelium was decreased compared with those from embryonic forebrain (Fig. 2A) and the diameter of the primary, secondary, tertiary neurosphere was smaller compared with those derived from embryonic forebrain (Fig. 2B), suggesting that the ciliary epithelium derived-neurospheres proliferate poorly.

Because Nestin expression is known to decrease gradually upon differentiation (Reynolds et al., 1992), we speculated that cells in a more differentiated state lose its expression more rapidly compared to the cells in an undifferentiated state. Hence, we sought to determine whether the percent of Nestin negative cells are different between progenitors from ciliary epithelium and embryonic forebrain. Although almost all the cells within the neurospheres expressed Nestin, neurosphere-forming cells from the ciliary epithelium showed tendency to lose Nestin

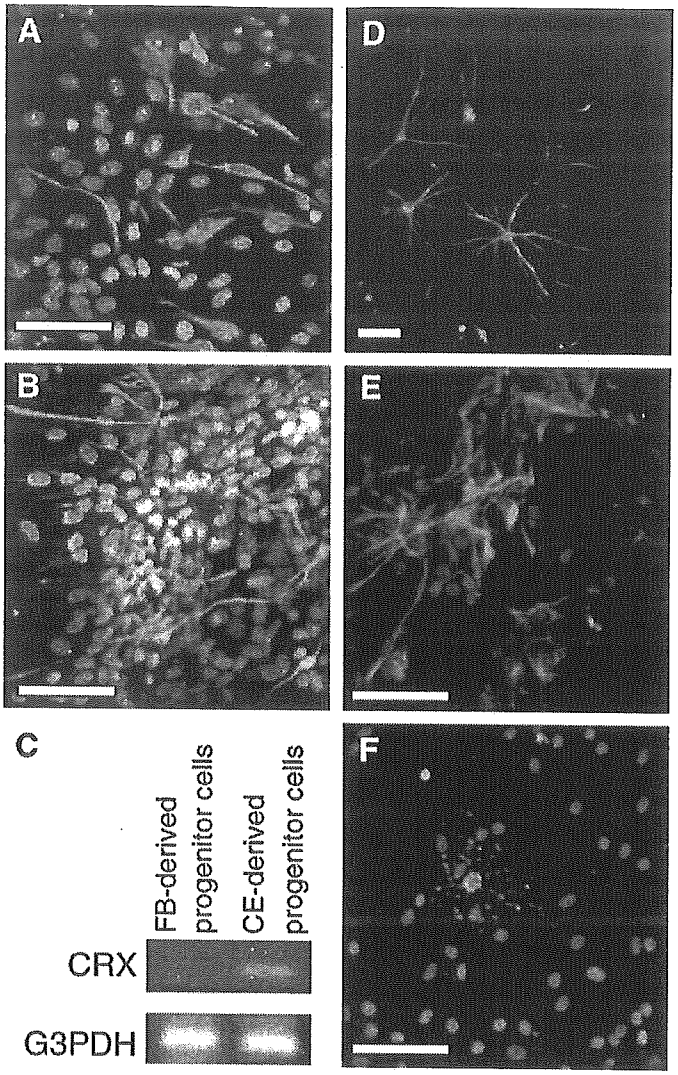

Fig. 1. Potential of differentiation of the progenitors derived from ciliary epithelium and embryonic forebrain. (A, B, D, E and F) Immunocytochemistry of the progenies derived from CE-derived retinal progenitor cells (A and B) and FB-derived progenitor cells (D–F). Both progenitors generate NF-M-positive putative neurons (A and D), GFAP-positive glia (B and E). FB-derived progenitor cells also generate O4-positive oligodendrocyte (F). The nucleus is counterstained with Hoechst 33258 and is depicted in blue. (C) RT-PCR analysis demonstrates that adult CE-derived retinal progenitor cells express CRX, whereas FB-derived progenitor cells do not. Note that the potency of differentiation of the progenies from the ciliary epithelium and embryonic forebrain are different in terms of the marker gene expressions and their morphology (see text for details.)

expression compared with the embryonic forebrain derived neurosphere forming cells when evaluated by immunocytochemistry 24 h after plating in the differentiating condition (Table 1). Next, we examined Notch signaling pathway molecules and other transcription factors that are considered as core factors defining the 'stemness' (Ramalho-Santos et al., 2002) by means of semi-quantitative RT-PCR using the secondary and passage 4 neurospheres from the ciliary epithelium. The result demonstrated that the expressions of several core factors defining stemness such as CyclinD1, Pten, ERCC-5 were not perturbed, while the expressions of Notch signaling pathway molecules, including Delta1, Notch1 and HES-5, were decreased in the passage 4 neurospheres compared with the passage 2 neurospheres (Fig. 3). Although the expression of a downstream effector of Notch signaling pathway, HES-1, was not decreased in the passage 4 neurospheres, these results demonstrated that the CE-derived neurospheres initially express the set of genes implicated in the maintenance of stem cells at least partly, but lose their expression after passaging. Taken together, CE-derived neurospheres contained fewer undifferentiated cells and more differentiated cells compared with the embryonic forebrain-derived neurospheres, and the undifferentiated cells within the neurospheres from the ciliary epithelium were reduced after passaging.

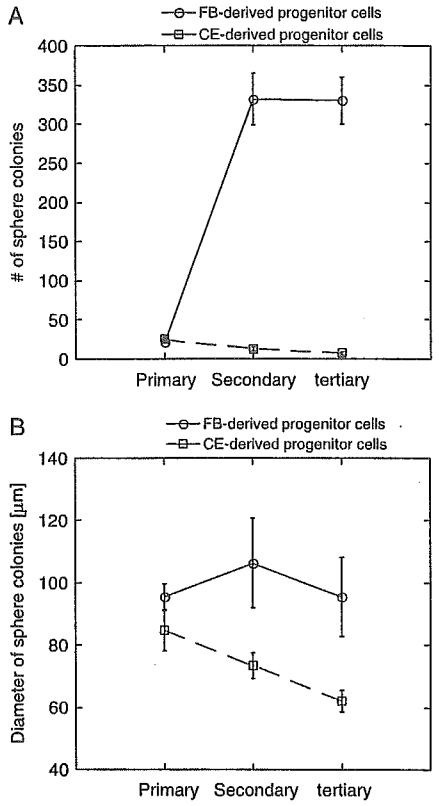

Fig. 2. Number and diameter of neurosphere colonies derived from embryonic forebrain and ciliarly epithelium. Sphere colonies obtained after 7 days in culture were collected, dissociated into single cells by trypsinization, plated 24 well dishes at a cell density 10 cells/μl in 24 well dish plates and cultured for further 7 days under the same condition. Cells were passaged every 7 days thereafter. (A) The number of neurosphere colonies per well was counted to give the value for one experiment. The data are mean from 6 experiments; error bars indicate S.E.M. (B) To measure the diameter of the neurosphere colonies, the cultures were observed with an inverted microscope and the images were analyzed by NIH image program. The diameter of at least 50 sphere colonies was measured. The data are mean from 6 experiments; error bars indicate S.E.M. Note that the neurospheres from the embryonic forebrain generate more neurosphres and are more proliferative compared with those derived from ciliary tpithelium. FB; forebrain, CE; ciliary epithelium.

Table 1
Precentage of Nestin positive cells 24 h after plating onto poly-L-lys/lamin coated dishes in the presence of 1% FBS

	Primary	Secondary	Tertiary
N	12	12	1
Neurospheres from the ciliary epithelium	93.7±3.5	64.6±3.5	67.8
N	3	3	3
Neurospheres from the embryonic forebrain	100±0.0	100±0.0	100±0.0

Data are presented as mean±SEM. The cells from the neurosphre were dissociated and plated onto poly-L-lys/laminine coated dishes. They were evaluated by immunocytochemistry 24 h after plating in the differentiating condition.

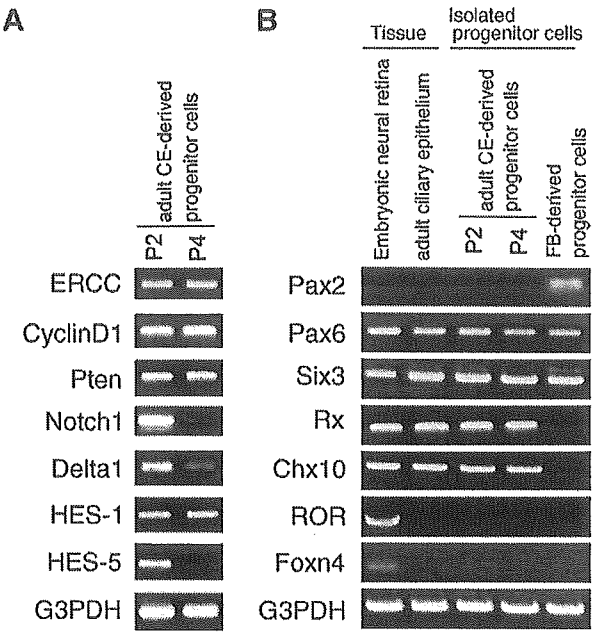

Fig. 3. Regulation of undifferentiated cell markers and transcription factors of the progenitors derived from ciliary epithelium during culture. (A) Expression levels of core stem cell factors including CyclinD1, Pten, ERCC-5, and Notch pathway singnaling molecules, Delta1, Notch1, HES-1 and HES-5, were examined by means of semi-quantitative RT-PCR using the secondary and passage 4 CE-derived retinal progenitor cells. Note that the expression levels of Delta1, Notch1 and HES-5 are decreased in the passage 4 progenitors. (B) Expressions of homeodomein factors including Pax2, Pax6, Six3, Rx and Chx10, and region-specific factors, RORβ and Foxn4 were examined using the mRNA from the ciliary epithelium and embryonic neural retina, and CE- and FB-derived progenitor cells. Three independent experiments were performed, which gave identical results. CE; ciliary epithelium, FB; forebrain, P2; passgage 2, P4; passage 4.

4. Expression of region specific transcription factors in progenitors from rat ciliary epithelium and embryonic forebrain

The potential of differentiation and proliferation of the progenitors from the ciliary epithelium differs from that of the progenitors from the embryonic forebrain (Fig. 1), raising the possibility that each progenitor expresses different sets of genes. Thus, we analyzed region-specific transcriptional factors expressed in the progenitors from the ciliary epithelium and embryonic forebrain. Concomitantly, we examined whether these factors are expressed in the embryonic day 17.5 neural retina and the adult ciliary epithelium. First, expressions of homeodomain factors including Pax2, Pax6, Six3, Rx and Chx10 were examined (Fig. 3B). The embryonic retina expressed Pax6, Six3, Rx and Chx10 as expected. The adult ciliary epithelium also expressed Pax6, Six3, Rx and Chx10. Neither embryonic retinal cells nor adult ciliary epithelium expressed Pax2. Progenitors from the ciliary epithelium expressed Pax6, Six3, Rx and Chx10 even after passaging, but not Pax2, whereas progenitors from the embryonic forebrain

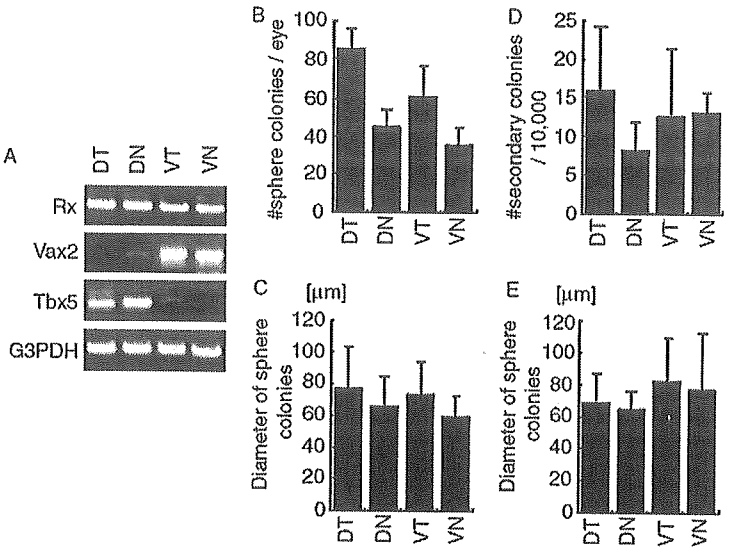

Fig. 4. Growth and molecular properties of sphere colonies from the ciliary epithelium subdivided into four subregions. (A) RT-PCR showing the expression pattern of Vax2 and Tbx5 before culture, suggesting that the eye was precisely divided along its dorsoventral and nasotemporal axes. (B and D) The number of primary (B) and secondary (D) neurosphere colonies per well was counted to give the value for one experiment. The data are mean from 6 experiments; error bars indicate S.E.M. (C and E) To measure the diameter of the primary (C) and secondary (E) neurosphere colonies, the cultures were observed with an inverted microscope and the images were analyzed by NIH image program. The diameter of at least 50 sphere colonies was measured. The data are mean from 6 experiments; error bars indicate S.E.M. D; dorsal, N; nasal, T; temporal, V; ventral

expressed Pax2, Pax6 and Six3, but not Rx and Chx10. Next, expressions of retinal specific transcription factors including RORβ and Foxn4 were examined (Fig. 3B). The embryonic retina expressed RORβ and Foxn4 as expected. However, the adult ciliary epithelium expressed neither of them. Neither progenitors from the ciliary epithelium nor embryonic forebrain expressed RORβ and Foxn4.

Next, we subdivided the CE into four subdivisions along its dorsoventral and nasotemporal axes and examined the sphere formation from these subdomains. To confirm the eye was precisely divided along its axes, the expression of dorsoventral markers markers, i.e. Vax2 and Tbx5, were examined before culturing (Fig. 4A). Interestingly, there was a trend for the ciliary epithelium from the temporal side to generate a greater number of colonies with larger diameter (Fig. 4B). The number and diameter of the secondary colonies from each subregion was similar (Fig. 4C). RT-PCR demonstrated that neither the primary and secondary colonies nor their progeny expressed detectable levels of Vax2 and Tbx5.

5. Discussion

Previous studies demonstrated that neural progenitor cells are present in the adult ciliary epithelium (Ahmad et al., 2000; Tropepe et al., 2000). In the current study, we isolated CE-derived retinal progenitor cells from adult rat ciliary epithelium (adult CE-derived retinal progenitor cells) using reaggregation-free methylcellulose gel matrix. Under our condition, it was not determined whether these progenitor cells from the ciliary epithelium possessed the properties of stem cells in vitro. Instead, our results support that the neurospheres from the ciliary epithelium contained fewer undifferentiated cells compared with the neurospheres from the embryonic forebrain, for several reasons. First, the number of neurosphere-initiating cells in the nuerospheres from the ciliary epithelium was few relative to those from the embryonic forebrain. Second, although the expression of Nestin was detected almost all the cells within the neurospheres, the number of Nestin positive cells was decreased compared to the embryonic forebrain-derived neurospheres when evaluated 24 h after differentiation. In addition, our results demonstrated that the relative expression levels of several components of the Notch pathway signaling molecules were decreased after the passaging of the neurospheres from the ciliary epithelium, suggesting that the undifferentiated cells within the neurospheres were reduced after passaging. To maintain retinal progenitor cells in an undifferentiated state in vivo, Notch signaling pathway molecules, such as Delta 1, Notch1, HES-1 and Hes-5 are essential. Lack of either gene in mice causes retinal progenitor cells to differentiate immaturely. (Bao and Cepko, 1997; Ohtsuka et al., 1999; Tomita et al., 1996) Taken together, our results demonstrated that the neurospheres from the ciliary epithelium contained fewer undifferentiated cells compared to the embryonic forebrain-derived neurospheres in rats.

We explored molecular properties of adult CE-derived retinal progenitor cells. Embryonic or postnatal retinal progenitor cells express regulatory molecules such as Pax6, Rx, Chx10, Foxn4 and RORβ in vivo (Chow et al., 1998;

Furukawa et al., 1997; Gouge et al., 2001; Liu et al., 1994; Marquardt et al., 2001; Mathers et al., 1997). In addition, expression of Pax2 and Six3 is detected in the developing neural retina (Dressler et al., 1990; Oliver et al., 1995). In the adult ciliary epithelium, we found that Pax6, Rx, Six3 and Chx10 are expressed. We have demonstrated that expression of these transcription factors can be recapitulated in vitro, i.e. CE-derived retinal progenitor cells express Pax6, Six3, Rx and Chx10. Even after passaging, expressions of these factors are retained, suggesting that their expression is not confined within the Notch1-positive undifferentiated progenitor cells in vitro. In the ventricular zone where forebrain neural progenitor cells are localized, expressions of Pax2, Pax6, Six3, Rx, Chx10 and RORβ are detected from the early stage of neurulation to immediately after optic vesicle evangination (Chow et al., 1998; Dressler et al., 1990; Furukawa et al., 1997; Gouge et al., 2001; Liu et al., 1994; Marquardt et al., 2001; Mathers et al., 1997; Oliver et al., 1995). However, expressions of Rx, Chx10, RORβ and Foxn4 fade in the late embryonic period (Chow et al., 1998; Furukawa et al., 1997; Gouge et al., 2001; Liu et al., 1994). In agreement with this, we found that the Pax6 and Six3 can be detected in the neurospheres from the E14 embryonic forebrain, but expressions of Rx, Chx10 RORβ and Foxn4 were not detected. Thus, adult CE-derived retinal progenitor cells in vitro express, at least to some extent, similar a set of transctription factors from the proliferatve retinal progenitors in vivo (Chow et al., 1998; Furukawa et al., 1997; Gouge et al., 2001; Liu et al., 1994; Marquardt et al., 2001; Mathers et al., 1997), which are different from those expressed in forebrain-derived neural progenitor cells. This is in good accordance with the previous studies demonstrating that the isolated neural stem cells from spinal cord (Yamamoto et al., 2001) or different regions of brain (Hitoshi et al., 2002) express different regional markers after culturing. Although further studies are necessary, it is tempting to speculate that such region-specific transcription factors might regulate the potential of differentiation of the progenitor cells.

We also found different properties between adult CE-derived retinal progenitor cells and embryonic or postnatal retinal progenitor cells in vivo in the following aspects. First, most embryonic retinal progenitor cells in vivo are considered multipotent and produce most of the cells in the neural retina (Cepko et al., 1996). However, adult CE-derived retinal progenitor cells did not generate neurons expressing markers specific for retinal ganglion cells and amacrine cells in vitro. Second, embryonic proliferative retinal progenitor cell cultures usually contain morphologically undifferentiated cells and principally two differentiated cells, i.e. multipolar neurons and photorecepotors having one short neurite (Kelley et al., 1995; Stenkamp and Adler, 1993). On the contrary, most of the neurons from the adult ciliary epithelium are bipolar. This is good accordance with previous studies (Ahmad et al., 2000; Tropepe et al., 2000); the differentiated progenies from the CE-derived retinal progenitor cells from mice and rats are stained with the some retinal selective markers, however, their morphologies seem different from those observed in embryonic retinal cultures (Kelley et al., 1995; Stenkamp and Adler, 1993). In addition, progenitor cells derived from the ciliary epithelium do not express transcription factors, such as RORβ and Foxn4 that in vivo proliferatve retinal progenitor cells express. Moreover, subregion analysis demonstrated that retinal progenitor cells did not express detectable levels of subregion specific transcription factors such as Vax2 and Tbx5. Thus, our results suggest that CE-derived retinal progenitors may have intrinsic limitations in the production of cell types.

Recent studies have shown that growth factor can induce neurogeneis in vivo in the CE cells. (Fischer and Reh, 2000) Furthermore, many of the molecular markers used to define differentiated retinal cells in vitro, such as markers from the phototransduction pathway or retinoid pathways, are already expressed in vivo and in vitro in adult CE cells (Bertazolli-Filho et al., 2001; Ghosh et al., 2004; Salvador-Silva et al., 2005), raising the possibility that adult CE, in vivo, may not contain retinal progenitor or stem cells, and that the cell and molecular characteristics, in vitro, described in this work as well as in previous studies, may simply reflect the embryological neural origin of the CE and its embryological relationship with the retina.

In summary, our study confirmed the previous studies that retinal progenitor cells can be isolated from the ciliary epithelium using reaggregation-free methylcellulose medium. As demonstrated in this study, CE-derived retinal progenitor cells contain fewer undifferentiated cells have limited capacity of self-renewal and lack the ability to produce specific types of retinal neurons in vitro. Despite these limitations, CE-derived retinal progenitor cells may be an attractive source of transplantation therapy for retinal diseases. Indeed, a recent study demonstrated that the CE-derived retinal progenitor cells can be incorporated into the injured retina and differentiate to mature retinal neurons (Chacko et al., 2003). To facilitate growth and/or differentiation of CE-derived retinal progenitor cells and to utilize CE-derived retinal progenitor cells as a cell-source of retinal repair, further studies regarding factors regulating their differentiation are necessary.

References

Ahmad, I., Tang, L., Pham, H., 2000. Identification of neural progenitors in the adult mammalian eye. Biochem Biophys Res Commun 270, 517–521.

Bao, Z.Z., Cepko, C.L., 1997. The expression and function of Notch pathway genes in the developing rat eye. J Neurosci 17, 1425–1434.

Barbieri, A.M., Broccoli, V., Bovolenta, P., Alfano, G., Marchitiello, A., Mocchetti, C., Crippa, L., Bulfone, A., Marigo, V., Ballabio, A., Banfi, S., 2002. Vax2 inactivation in mouse determines alteration of the eye dorsal-ventral axis, misrouting of the optic fibres and eye coloboma. Development 129, 805–813.

Bertazolli-Filho, R., Ghosh, S., Huang, W., Wollmann, G., Coca-Prados, M., 2001. Molecular evidence that human ocular ciliary epithelium expresses components involved in phototransduction. Biochem Biophys Res Commun 284, 317–325.

Burmeister, M., Novak, J., Liang, M.Y., Basu, S., Ploder, L., Hawes, N.L., Vidgen, D., Hoover, F., Goldman, D., Kalnins, V.I., Roderick, T.H., Taylor, B.A., Hankin, M.H., McInnes, R.R., 1996. Ocular retardation mouse caused by Chx10 homeobox null allele: impaired retinal progenitor proliferation and bipolar cell differentiation. Nat Genet 12, 376–384.

Cepko, C.L., Austin, C.P., Yang, X., Alexiades, M., Ezzeddine, D., 1996. Cell fate determination in the vertebrate retina. Proc Natl Acad Sci U S A 93, 589–595.

Chacko, D.M., Das, A.V., Zhao, X., James, J., Bhattacharya, S., Ahmad, I., 2003. Transplantation of ocular stem cells: the role of injury in incorporation and differentiation of grafted cells in the retina. Vision Res 43, 937–946.

Chow, L., Levine, E.M., Reh, T.A., 1998. The nuclear receptor transcription factor, retinoid-related orphan receptor beta, regulates retinal progenitor proliferation. Mech Dev 77, 149–164.

Dressler, G.R., Deutsch, U., Chowdhury, K., Nornes, H.O., Gruss, P., 1990. Pax2, a new murine paired-box-containing gene and its expression in the developing excretory system. Development 109, 787–795.

Fischer, A.J., Reh, T.A., 2000. Identification of a proliferating marginal zone of retinal progenitors in postnatal chickens. Dev Biol 220, 197–210.

Furukawa, T., Kozak, C.A., Cepko, C.L., 1997. rax, a novel paired-type homeobox gene, shows expression in the anterior neural fold and developing retina. Proc Natl Acad Sci U S A 94, 3088–3093.

Ghosh, S., Salvador-Silva, M., Coca-Prados, M., 2004. The bovine iris-ciliary epithelium expresses components of rod phototransduction. Neurosci Lett 370, 7–12.

Gouge, A., Holt, J., Hardy, A.P., Sowden, J.C., Smith, H.K., 2001. Foxn4–a new member of the forkhead gene family is expressed in the retina. Mech Dev 107, 203–206.

Gritti, A., Frolichsthal-Schoeller, P., Galli, R., Parati, E.A., Cova, L., Pagano, S.F., Bjornson, C.R., Vescovi, A.L., 1999. Epidermal and fibroblast growth factors behave as mitogenic regulators for a single multipotent stem cell-like population from the subventricular region of the adult mouse forebrain. J Neurosci 19, 3287–3297.

Gritti, A., Parati, E.A., Cova, L., Frolichsthal, P., Galli, R., Wanke, E., Faravelli, L., Morassutti, D.J., Roisen, F., Nickel, D.D., Vescovi, A.L., 1996. Multipotential stem cells from the adult mouse brain proliferate and self-renew in response to basic fibroblast growth factor. J Neurosci 16, 1091–1100.

Gruss, P., Walther, C., 1992. Pax in development. Cell 69, 719–722.

Hitoshi, S., Tropepe, V., Ekker, M., van der Kooy, D., 2002. Neural stem cell lineages are regionally specified, but not committed, within distinct compartments of the developing brain. Development 129, 233–244.

Inoue, Y., Yanagi, Y., Tamaki, Y., Uchida, S., Kawase, Y., Araie, M., and Okochi, H. (2005). Clonogenic analysis of ciliary epithelial derived retinal progenitor cells in rabbits. in press.

Kawase, Y., Yanagi, Y., Takato, T., Fujimoto, M., Okochi, H., 2004. Characterization of multipotent adult stem cells from the skin: transforming growth factor-beta (TGF-beta) facilitates cell growth. Exp Cell Res 295, 194–203.

Kelley, M.W., Turner, J.K., Reh, T.A., 1995. Ligands of steroid/thyroid receptors induce cone photoreceptors in vertebrate retina. Development 121, 3777–3785.

Liu, I.S., Chen, J.D., Ploder, L., Vidgen, D., van der Kooy, D., Kalnins, V.I., McInnes, R.R., 1994. Developmental expression of a novel murine homeobox gene (Chx10): evidence for roles in determination of the neuroretina and inner nuclear layer. Neuron 13, 377–393.

Marquardt, T., Ashery-Padan, R., Andrejewski, N., Scardigli, R., Guillemot, F., Gruss, P., 2001. Pax6 is required for the multipotent state of retinal progenitor cells. Cell 105, 43–55.

Mathers, P.H., Grinberg, A., Mahon, K.A., Jamrich, M., 1997. The Rx homeobox gene is essential for vertebrate eye development. Nature 387, 603–607.

Morshead, C.M., Reynolds, B.A., Craig, C.G., McBurney, M.W., Staines, W.A., Morassutti, D., Weiss, S., van der Kooy, D., 1994. Neural stem cells in the adult mammalian forebrain: a relatively quiescent subpopulation of subependymal cells. Neuron 13, 1071–1082.

Nornes, H.O., Dressler, G.R., Knapik, E.W., Deutsch, U., Gruss, P., 1990. Spatially and temporally restricted expression of Pax2 during murine neurogenesis. Development 109, 797–809.

Ohtsuka, T., Ishibashi, M., Gradwohl, G., Nakanishi, S., Guillemot, F., Kageyama, R., 1999. Hes1 and Hes5 as notch effectors in mammalian neuronal differentiation. Embo J 18, 2196–2207.

Oliver, G., Mailhos, A., Wehr, R., Copeland, N.G., Jenkins, N.A., Gruss, P., 1995. Six3, a murine homologue of the sine oculis gene, demarcates the most anterior border of the developing neural plate and is expressed during eye development. Development 121, 4045–4055.

Pittman, A., Chien, C.B., 2002. Understanding dorsoventral topography: backwards and forwards. Neuron 35, 409–411.

Ramalho-Santos, M., Yoon, S., Matsuzaki, Y., Mulligan, R.C., Melton, D.A., 2002. 'Stemness' : transcriptional profiling of embryonic and adult stem cells. Science 298, 597–600.

Reynolds, B.A., Tetzlaff, W., Weiss, S., 1992. A multipotent EGF-responsive striatal embryonic progenitor cell produces neurons and astrocytes. J Neurosci 12, 4565–4574.

Reynolds, B.A., Weiss, S., 1996. Clonal and population analyses demonstrate that an EGF-responsive mammalian embryonic CNS precursor is a stem cell. Dev Biol 175, 1–13.

Salvador-Silva, M., Ghosh, S., Bertazolli-Filho, R., Boatright, J.H., Nickerson, J.M., Garwin, G.G., Saari, J.C., Coca-Prados, M., 2005. Retinoid processing proteins in the ocular ciliary epithelium. Mol Vis 11, 356–365.

Schulte, D., Furukawa, T., Peters, M.A., Kozak, C.A., Cepko, C.L., 1999. Misexpression of the Emx-related homeobox genes cVax and mVax2 ventralizes the retina and perturbs the retinotectal map. Neuron 24, 541–553.

Stenkamp, D.L., Adler, R., 1993. Photoreceptor differentiation of isolated retinal precursor cells includes the capacity for photomechanical responses. Proc Natl Acad Sci U S A 90, 1982–1986.

Tomita, K., Ishibashi, M., Nakahara, K., Ang, S.L., Nakanishi, S., Guillemot, F., Kageyama, R., 1996. Mammalian hairy and Enhancer of split homolog 1 regulates differentiation of retinal neurons and is essential for eye morphogenesis. Neuron 16, 723–734.

Tropepe, V., Coles, B.L., Chiasson, B.J., Horsford, D.J., Elia, A.J., McInnes, R.R., van der Kooy, D., 2000. Retinal stem cells in the adult mammalian eye. Science 287, 2032–2036.

Yamamoto, S., Nagao, M., Sugimori, M., Kosako, H., Nakatomi, H., Yamamoto, N., Takebayashi, H., Nabeshima, Y., Kitamura, T., Weinmaster, G., Nakamura, K., Nakafuku, M., 2001. Transcription factor expression and Notch-dependent regulation of neural progenitors in the adult rat spinal cord. J Neurosci 21, 9814–9823.

The Effects of Prostaglandin Analogues on IOP in Prostanoid FP-Receptor–Deficient Mice

Takashi Ota,[1] *Makoto Aihara,*[1] *Shuh Narumiya,*[2] *and Makoto Araie*[1]

Purpose. This study was designed to clarify the involvement of the prostanoid FP receptor in the intraocular pressure (IOP)-lowering effects of latanoprost, travoprost, bimatoprost, and unoprostone with the use of FP-receptor-deficient (FPKO) mice.

Methods. FPKO and wild-type (WT) mice were bred and acclimatized under a 12-hour light-dark cycle. IOP was measured under general anesthesia by a microneedle method. To evaluate the effects of each drug, a single drop (3 μL) of each drug solution was topically applied in a masked manner to a randomly selected eye. IOP reduction was evaluated by the difference in IOP between the treated eye and the untreated contralateral eye in the same mouse. First, the diurnal variation and baseline IOP in WT and FPKO mice were measured. Then, to determine the window feasible for demonstrating the most marked ocular hypotensive effect, 0.005% latanoprost was applied to WT mice during the day or at night. The time when the ocular hypotensive effect was larger was selected for further studies to evaluate the effects of latanoprost (0.005%), travoprost (0.004%), bimatoprost (0.03%), and unoprostone (0.12%). In addition, bunazosin (0.1%) was also applied to demonstrate functional uveoscleral outflow in FPKO mice. All experiments were conducted under a masked study design.

Results. The baseline IOP (mean ± SEM) in WT and FPKO mice was 15.0 ± 0.2 and 15.0 ± 0.3 mm Hg, respectively, during the day, and 18.9 ± 0.4 and 19.2 ± 0.4 mm Hg, respectively, at night. In WT mice, latanoprost significantly lowered IOP both during the day and at night, at 2 to 6 hours and 1 to 6 hours after application, respectively. Maximal IOP reduction was observed at 3 hours after drug instillation both during the day (10.9 ± 1.8%) and at night (23.2 ± 1.1%). At 3 hours after instillation, latanoprost (10.9 ± 1.8% and 23.2 ± 1.1%, daytime and nighttime, respectively), travoprost (15.9 ± 1.4% and 26.1 ± 1.2%) and bimatoprost (8.8 ± 2.0 and 19.8 ± 1.5%) significantly lowered IOP in WT mice both during the day and at night; isopropyl unoprostone significantly lowered IOP at night (13.7 ± 1.9%) but not during the day (5.3 ± 3.2%). In FPKO mice, latanoprost, travoprost, bimatoprost, and unoprostone showed no significant IOP-lowering effect. Bunazosin significantly lowered IOP in both WT (22.1 ± 1.6%) and FPKO mice (22.2 ± 2.1%).

Conclusions. A single application of latanoprost, travoprost, bimatoprost, or unoprostone had no effect on IOP in FPKO mice with presumed functional uveoscleral outflow pathways. The prostanoid FP receptor plays a crucial role in the mechanism of early IOP lowering of all commercially available prostaglandin analogues. (*Invest Ophthalmol Vis Sci.* 2005;46:4159-4163) DOI:10.1167/iovs.05-0494

Prostaglandin (PG) analogues have been widely used as ocular hypotensive drugs for the treatment of glaucoma and ocular hypertension, because of both a greater effect in lowering intraocular pressure (IOP) and fewer systemic side effects than β-blockers. Currently, four different types of PG analogues, latanoprost, travoprost, bimatoprost, and isopropyl unoprostone (unoprostone), are used for the treatment of glaucoma. Latanoprost and travoprost are thought to lower IOP mainly via the FP receptor because of their high degree of specificity to this receptor.[1] This is supported by a recent report that latanoprost showed no IOP-lowering effect in FP-receptor-deficient (FPKO) mice.[2] On the other hand, the IOP-lowering mechanisms of bimatoprost and unoprostone are not fully understood.

Bimatoprost, which has the structure of a prostamide, was originally reported not to act as a PG analogue because of not binding to all prostanoid receptors.[3] So far, no specific receptor for bimatoprost has been determined. However, its metabolite, bimatoprost free acid, binds to the FP receptor with a potency similar to that of latanoprost.[1,4-11] Recently, bimatoprost has been shown to be readily hydrolyzed to the free acid in human eyes[12] (Dahlin DC. *IOVS* 2004;45:ARVO E-Abstract 2096). In addition, bimatoprost itself has a weak affinity to FP, leading to increased intracellular calcium concentration.[7] Thus, bimatoprost may exert FP agonistic activity.

Unoprostone shows low affinities for all prostanoid receptors.[1] However, there are several hypotheses to explain unoprostone-induced IOP reduction. Unoprostone free acid and further metabolites have been reported to stimulate PGE_2 release, which may play a role in IOP reduction by unoprostone.[13,14] Unoprostone free acid activates maxi-K channels to inhibit trabecular meshwork contraction, which can lead to increases in aqueous outflow.[15] Finally, unoprostone can induce cellular responses similar to those induced by other FP agonists in cultured ciliary muscle cells and trabecular meshwork cells, probably by acting as a weak FP agonist.[1,5,7,8]

The discrepancies in many reports may be due to the limitations of the results generated by pharmacological in vitro experiments. For this reason, the transgenic mouse is a powerful tool for investigating single-gene-related function in vivo. In an attempt to shed light on the IOP-lowering mechanism of bimatoprost and unoprostone and to confirm the FP-receptor-mediated action of latanoprost and travoprost, we examined the effects of four commercially available PG analogues, latanoprost, travoprost, bimatoprost, and unoprostone, on IOP in prostanoid FP-receptor-deficient mice. In addition, the response to bunazosin HCl, which has been reported to decrease IOP by increasing uveoscleral outflow,[16,17] was measured to establish the presence of functional uveoscleral outflow pathways in FPKO mice.

From the [1]Department of Ophthalmology, University of Tokyo School of Medicine, Tokyo, Japan; and the [2]Department of Pharmacology, Kyoto University, Faculty of Medicine, Kyoto, Japan.

Supported in part by Grant-in-Aid for Science Research A-14207049 from the Japanese Ministry of Education, Culture, Sports, Science, and Technology (MAr).

Submitted for publication April 21, 2005; revised July 3, 2005; accepted September 14, 2005.

Disclosure: **T. Ota**, None; **M. Aihara**, None; **S. Narumiya**, None; **M. Araie**, None

The publication costs of this article were defrayed in part by page charge payment. This article must therefore be marked "*advertisement*" in accordance with 18 U.S.C. §1734 solely to indicate this fact.

Corresponding author: Makoto Aihara, Department of Ophthalmology, University of Tokyo School of Medicine, 7-3-1 Hongo Bunkyo-ku Tokyo 113-8655, Japan; aihara-tky@umin.ac.jp.

Materials and Methods

Animals

All experiments were performed in compliance with the ARVO Statement for the Use of Animals in Ophthalmic and Vision Research. FPKO mice were generated by homologous recombination with a target vector that replaces the second exon of the FP gene with the β-galactosidase- and neomycin-resistant gene. Homozygous knockout mice do not transcribe FP-receptor mRNA.[18] Both homozygous and heterozygous knockout mice develop normally, and have no gross abnormalities in behavior, macro- or microscopic anatomy, or biochemical or hematologic indices.[18] Because homozygote knockout females fail to initiate parturition, heterozygous (female) and homozygous (male) mating pairs were used to generate an F1 generation. Murine genotype was determined by PCR,[2] and FP-receptor homozygous knockout mice were used. C57BL/6 mice, which constitute the background species of the FPKO mice, were used as the wild-type (WT) control. Mice were bred and housed in clear cages, loosely covered with air filters, and white chips provided bedding. The environment was kept at 21°C with a 12-hour light (6 AM to 6 PM) and 12-hour dark cycle. All mice were fed ad libitum and acclimatized to the environment for at least 2 weeks before the experiments. We used mice older than 8 weeks of age in our study.

Preparation and Instillation of Ophthalmic Solution

Latanoprost and bimatoprost were purchased from Cayman Chemical Co. (Ann Arbor, MI). Latanoprost (0.005%) was dissolved in its vehicle solution as reported previously.[19] Bimatoprost (0.03%) was dissolved in phosphate-buffered saline (PBS). Travoprost (0.004%), unoprostone (0.12%), and bunazosin HCl (0.1%) ophthalmic solutions, and the vehicle solution for each, were provided by Alcon Inc. (Fort Worth, TX), R-Tech Ueno Ltd. (Hyogo, Japan), and Santen Pharmaceutical (Osaka, Japan), respectively. With a micropipette, 3 μL of each drug solution was topically applied in a masked manner to a randomly selected eye, and the contralateral, untreated eye served as the control.

IOP Measurement

IOP was measured by a microneedle method in mice anesthetized with ketamine and xylazine, as described previously.[20] Briefly, a borosilicate glass microneedle (100-μm tip diameter and 1.0-mm outer diameter; World Precision Instruments [WPI], Sarasota, FL) was connected to a pressure transducer (Model BLPR; WPI). The system pressure detected by the transducer was recorded by a data acquisition and analysis system (PowerLab; ADInstruments, Colorado Springs, CO). The microneedle was placed in the anterior chamber, and the conducted pressure was recorded in both eyes during a 4- to 7-minute time window after anesthesia. Until the mouse was placed on the table for IOP measurement, room lighting was maintained similarly to that in the vivaria. For dark-phase measurements, all procedures were performed under red light illumination to eliminate the effect of lighting on IOP. The effect of each drug was calculated as the ratio of IOP reduction (%), defined as 100 × (IOP of treated eye − IOP of contralateral eye)/IOP of contralateral eye in each mouse.

Diurnal Variation of IOP in WT and FPKO Mice

Diurnal IOP variation in WT and FPKO mice was measured during the day (9 AM) and at night (9 PM) by a microneedle method in mice under general anesthesia. The time points for IOP measurement were chosen in accordance with previous reports.[20,21] Trough and peak IOP under the 12-hour light–dark cycle was observed at 9 AM and at 9 PM in NIH Swiss and ddY mice.

Time-Course Effect of Latanoprost on IOP in WT Mice

To determine the best time point for demonstrating the greatest ocular hypotensive effect of PG analogues, we evaluated the time course of latanoprost on IOP in WT mice. Three microliters of 0.005% latanoprost was applied to one randomly selected eye of an animal at 6 AM or 6 PM, and the IOP-lowering effect of latanoprost was measured at 1, 2, 3, and 6 hours after drug instillation, as previously reported.[21] The time point at which the ocular hypotensive effect was greatest was used for further studies to evaluate the effects of PG analogues.

Effect of Vehicle Solutions on IOP in WT and FPKO Mice

To confirm that the vehicle solutions did not affect IOP, 3 μL vehicle solution for each PG analogue and bunazosin was administrated topically to one randomly chosen eye in both WT and FPKO mice at 6 AM or 6 PM. Three investigators instilled eye drops under blinded test protocols. A fourth investigator, also masked to the treatment, measured IOP 3 hours after drug instillation, as described above. Thus, all measurements were performed under masked conditions.

IOP-Lowering Effects of PG Analogues on WT and FPKO Mice during the Day and at Night

Three microliters of latanoprost (0.005%), travoprost (0.004%), bimatoprost (0.03%), or isopropyl unoprostone (0.12%) was administrated topically to one randomly chosen eye in both WT and FPKO mice at 6 AM or 6 PM. Three investigators instilled eye drops under blinded test protocols. A fourth investigator, also masked to the treatment, measured IOP 3 hours after drug instillation, as described above. Thus, all measurements were performed under masked conditions.

IOP-Lowering Effect of Bunazosin HCl on WT and FPKO Mice at Night

Three microliters of bunazosin HCl (bunazosin; 0.1%) was topically applied to one randomly chosen eye in both WT and FPKO mice at 6 PM. The instillation and IOP measurement were performed under the masked conditions described above. At 3 hours after drug instillation, IOP was measured as described above.

Statistical Analysis

The Mann–Whitney *U* test was used for comparison of baseline IOP between daytime and nighttime values in each strain and also for comparison of IOP reduction between WT and FPKO mice. The Wilcoxon signed-ranks test was used for comparison of IOP between the treated eye and the contralateral eye. The Kruskal-Wallis test was used for multiple comparisons of IOP. Values of $P < 0.05$ were considered significant. All data are presented as means ± SEM.

Results

Diurnal Variation of Baseline IOP in WT and FPKO Mice

Mean IOP during the day (9 AM) and at night (9 PM) was 15.0 ± 0.2 and 18.9 ± 0.4 mm Hg, respectively, in WT mice, and 15.0 ± 0.3 and 19.2 ± 0.4 mm Hg, respectively, in FPKO

Table 1. Baseline IOP in WT and FPKO Mice during the Day and at Night

	IOP (mm Hg)	
Time Point	**WT**	**FPKO**
Day (9 AM)	15.0 ± 0.2 (11)	15.0 ± 0.3 (11)
Night (9 PM)	18.9 ± 0.4* (12)	19.2 ± 0.4* (10)

IOP was measured by a microneedle method under general anesthesia. Data are expressed as means ± SEM (*n*). There was no significant difference between WT and FPKO mice at either time point.

* Different from daytime (Mann–Whitney *U* test), $P < 0.0001$.

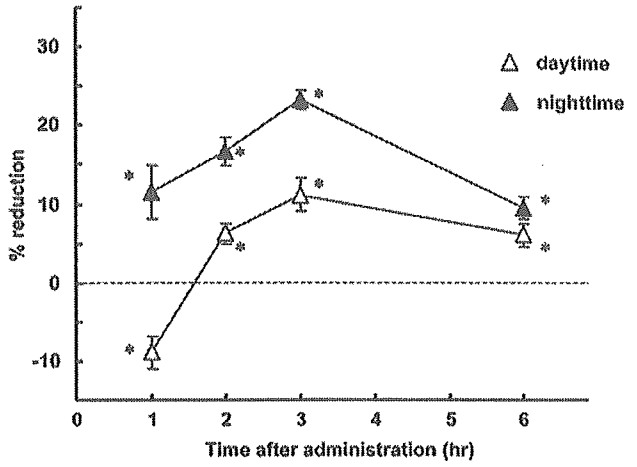

FIGURE 1. Effect of latanoprost (0.005%) on IOP in WT mice during the day and at night. Three microliters of latanoprost was topically applied at 6 AM or 6 PM, and IOP was measured at 1, 2, 3, and 6 hours after administration by a microneedle method under general anesthesia. Open and solid triangles indicate IOP reduction (%) during the day and at night, respectively. Data are expressed as means ± SEM (n = 7–11). *Different from untreated contralateral eye (Wilcoxon signed-ranks test), $P < 0.05$.

mice (Table 1). The nighttime IOP was significantly higher than the daytime IOP ($P < 0.0001$) for each genotype. However, there was no significant difference in IOP between genotypes, either during the day or at night.

Effect of Latanoprost on IOP in WT Mice during the Day and at Night

To confirm the effect of latanoprost on IOP in WT mice and to determine the best time point for comparison of PG-analogue hypotensive effects, we examined the IOP-lowering effect of latanoprost (0.005%) at 1, 2, 3, and 6 hours after drug instillation at 6 AM (daytime) and at 6 PM (nighttime) (Fig. 1). After drug application at 6 AM, a significant elevation in IOP (8.9 ± 2.1%, $P = 0.0069$) was seen at 1 hour, followed by significant reductions in IOP at 2 (5.9 ± 1.5%, $P = 0.0051$), 3 (10.9 ± 1.8%, $P = 0.0180$), and 6 hours (6.0 ± 1.7%, $P = 0.0125$). After drug application at 6 PM, latanoprost significantly lowered IOP at 1 (11.5 ± 3.3%, $P = 0.0069$), 2 (16.7 ± 1.8%, $P = 0.0051$), 3 (23.2 ± 1.1%, $P = 0.0033$), and 6 hours (9.5 ± 1.4%, $P = 0.0051$). There was no significant difference in mean baseline IOP of the contralateral eye among the four time points during the day ($P = 0.0720$) or at night ($P = 0.5790$). Maximal IOP reduction (both daytime and nighttime) was observed at 3 hours after latanoprost instillation. Therefore, comparisons of the IOP-lowering effects of PG analogues in the present study were made at 3 hour after drug administration, both during the day and at night.

Effect of Vehicle Solutions on IOP in WT and FPKO Mice

At 3 hours after treatment with each vehicle solution, the mean IOP reductions during the day and at night ranged from −2.0% to 1.6% and from −2.2% to 2.1%, respectively, in WT mice and from −1.9% to 2.1% and from −1.2% to 2.5%, respectively, in FPKO mice. None of the vehicle solutions showed a significant effect on IOP.

Effect of PG Analogues on IOP in WT and FPKO Mice during the Day and at Night

During the day, latanoprost (10.9 ± 1.8%, $P = 0.0117$), travoprost (15.9 ± 1.4%, $P = 0.0180$), and bimatoprost (8.7 ± 2.0%, $P = 0.0180$) significantly lowered IOP in WT mice (Fig. 2A), whereas these four drugs had no effect on IOP in FPKO mice (Fig. 3A). At night, latanoprost (23.2 ± 1.1%, $P = 0.0033$), travoprost (26.1 ± 1.2%, $P = 0.0051$), bimatoprost (19.8 ± 1.5%, $P = 0.0051$), and unoprostone (13.7 ± 1.9%, $P = 0.0051$) significantly lowered IOP in WT mice (Fig. 2B), whereas they had no significant effect on IOP in FPKO mice (Fig. 3B). In WT mice, the IOP-lowering effect of each PG analogue was greater at night than during the day (Figs. 2A and B); conversely, in FPKO mice, the IOP-lowering effects of PG analogues did not differ significantly between daytime and nighttime administration (Figs. 3A and B).

Effect of Bunazosin HCl on IOP in WT and FPKO Mice at Night

Bunazosin significantly lowered IOP at 3 hours after instillation in both WT (22.1 ± 1.6%, $P = 0.0033$) and FPKO mice (22.2 ± 2.1%, $P = 0.0051$) (Fig. 4). However, there was no significant difference in the magnitude of IOP reduction between WT and FPKO mice ($P = 0.7782$).

DISCUSSION

In this study, we examined the effects of PG analogues on IOP in FPKO mice. In the absence of the prostanoid FP receptor, the IOP-lowering effects of a single instillation of PG analogues including latanoprost, travoprost, bimatoprost, and unoprostone were completely eliminated. On the other hand, bunazosin, which lowers IOP by improving uveoscleral outflow,[16,17] lowered IOP in FPKO mice. Thus, FPKO mice do not likely have functional abnormalities in uveoscleral outflow. These results suggest that the prostanoid FP receptor plays a crucial role in the early IOP-lowering mechanism of all commercially available PG analogues. However, the intracellular signaling pathway and cellular response to FP-receptor binding have not

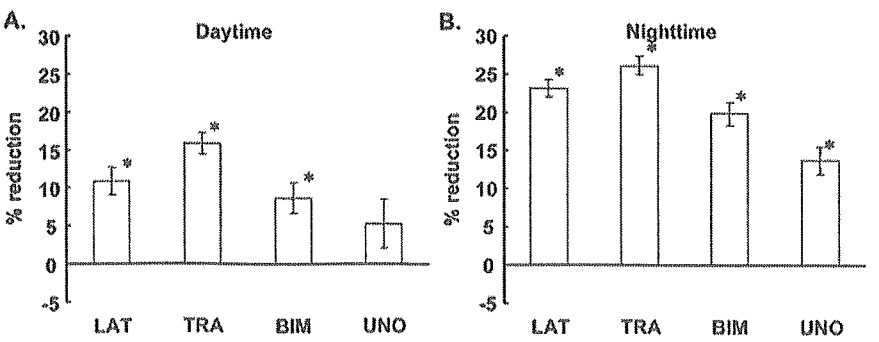

FIGURE 2. Effects of latanoprost (LAT, 0.005%), travoprost (TRA, 0.004%), bimatoprost (BIM, 0.03%), and isopropyl unoprostone (UNO, 0.12%) on IOP in WT mice. Three microliters of each drug was topically applied at 6 AM (A) or 6 PM (B), and IOP was measured at 3 hours after administration by a microneedle method under general anesthesia. Open columns indicate IOP reduction (%). Data are expressed as means ± SEM (n = 7–11). *Different from untreated contralateral eye (Wilcoxon signed-ranks test), $P < 0.05$.

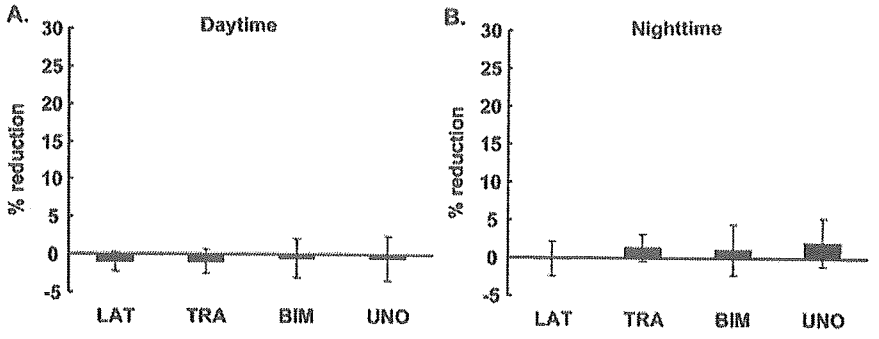

FIGURE 3. Effects of latanoprost (LAT, 0.005%), travoprost (TRA, 0.004%), bimatoprost (BIM, 0.03%), and isopropyl unoprostone (UNO, 0.12%) on IOP in FPKO mice. Three microliters of each drug was topically applied at 6 AM (A) or 6 PM (B), and IOP was measured at 3 hours after administration by a microneedle method under general anesthesia. Closed columns indicate IOP reduction (%). Data are expressed as means ± SEM (n = 8–10). No significant IOP reduction was observed (Wilcoxon signed-ranks test).

been fully clarified. Especially with regard to the short-term effect, there must be some cellular responses different from the induction of matrix metalloproteinase and the subsequent remodeling of extracellular matrices, which occur over a long time span.[22,23]

Our results confirm those of a previous study in which latanoprost failed to induce an IOP-lowering effect in FPKO and FP-receptor heterogeneous knockout mice; these mice had no obvious anatomic differences compared to WT mice.[2] In the previous study, however, IOP was measured during the day (between 2 and 6 PM), when IOP in the WT mice was not high (13.9–14.6 mm Hg), likely due to the 24-hour variation in IOP. Thus, the measured IOP reduction induced by latanoprost in the WT mice was small (−1.4 mm Hg) and not necessarily adequate for comparison with that in the FPKO mice. Moreover, only the structural similarity in the uveoscleral outflow pathway between FPKO and WT mice was histologically examined. In light of these previous results, the baseline IOP and the response to latanoprost were measured both during the day and at night, and the nighttime measurement was also adopted to detect the IOP response in FPKO mice. In addition, the functional integrity of the uveoscleral outflow pathway in FPKO was suggested by bunazosin.

Interestingly, bimatoprost and unoprostone completely failed to lower IOP in FPKO mice. Thus, bimatoprost and unoprostone may lower IOP in mice via their converted acid forms, which are bound to the FP receptor; this is supported by reports of previous in vitro studies.[1,4–11] Recent reports also indicate that bimatoprost can stimulate human FP receptors.[1,5,7,8] However, it is possible that FP agonists produced by bimatoprost and unoprostone act on FP receptors via unknown signal pathways. To clarify this issue, determination of PG analogues in the aqueous after instillation of bimatoprost and unoprostone in FPKO mice will be required.

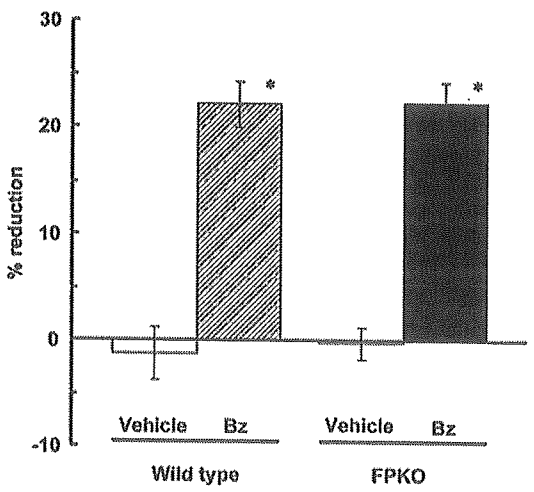

FIGURE 4. Effect of bunazosin HCl (Bz, 0.1%) on IOP in WT and FPKO mice. Three microliters of bunazosin HCl was topically applied at 6 PM, and IOP was measured at 3 hours after administration by a microneedle method under general anesthesia mice. Data are expressed as means ± SEM (n = 10 or 11). *$P < 0.05$ for treated versus untreated, contralateral eye (Wilcoxon signed-ranks test).

The mechanism of IOP reduction by bimatoprost has been thought to involve improvements in conventional and uveoscleral outflow pathways in monkeys and humans.[24,25] Thus, bimatoprost may also mediate IOP reduction via receptors other than FP receptors, which mainly affect the uveoscleral outflow pathway. Bimatoprost free acid can also bind to the EP1 receptor.[1] However, the absence of IOP reduction in FPKO mice suggests that the contributions of other receptors are limited, as far as the early IOP-lowering mechanism of bimatoprost is concerned.

Unoprostone may act as a weak FP agonist, despite having low affinities for all prostanoid receptors.[1] This is also supported by the cellular responses seen in cultured ciliary muscle cells and trabecular meshwork cells.[1,5,7,8] Stimulation of PGE_2 release by unoprostone free acid and further metabolites[13,14] may be unrelated to the IOP-lowering effect, at least in mice.

Travoprost significantly lowered IOP in WT mice both during the day and at night in the present study. These results are comparable with those of our previous study using ddY mice.[21] The absence of a travoprost-induced IOP-lowering effect in FPKO mice is an expected outcome considering its higher selectivity, potency, and affinity for the FP receptor compared to latanoprost.[5,7]

It must be noted that the present results involve the ocular hypotensive effect after a single instillation of a PG analogue in mice, which implies that direct extrapolation of the present results to humans or glaucoma patients may be difficult. Clinically it is well known that IOP reduction after a single instillation of latanoprost is not so remarkable as after once-daily long-term instillation. The mechanism of action after a single instillation may be different from that after long-term use. Ocular hypotensive effects by various PG analogues obtained in mice do not seem to parallel those in humans. In fact, the ocular hypotensive effect of latanoprost tended to be a little greater than that of bimatoprost in mice (Fig. 2), while previous studies suggested that the ocular hypotensive effect of bimatoprost tended to be a little greater than that of latanoprost in human patients.[26–29] In the present study, we demonstrated that IOP reduction after a single application of PG analogues in mice was FP-receptor dependent, suggesting that FP receptors are at least partly involved in the ocular hypotensive effect of latanoprost, travoprost, bimatoprost, or unoprostone in humans as well. Effects of bimatoprost or unoprostone in humans cannot be explained only by FP receptors. Therefore, further studies are required to clarify the involvement of

the FP receptor in IOP reduction with long-term administration of FP agonists.

Because IOP lowering is primarily mediated via FP receptors, it is an interesting question whether ocular side effects induced by PG analogues are also observed in FPKO mice. Since FPKO mice have similar IOP patterns and seemingly normal functional uveoscleral outflow pathways (both functionally and structurally), FPKO mice may be useful in developing new PG-analogue drugs with greater ocular hypotensive potential and lesser ocular side effects.

In conclusion, the finding that travoprost, bimatoprost, and isopropyl unoprostone, as well as latanoprost, failed to lower IOP in FPKO mice provides evidence that the FP receptor plays a critical role in the IOP-lowering effect of these PG analogues, at least as far as short-term effects are concerned.

References

1. Sharif NA, Kelly CR, Crider JY, Williams GW, Xu SX. Ocular hypotensive FP prostaglandin (PG) analogs: PG receptor subtype binding affinities and selectivities, and agonist potencies at FP and other PG receptors in cultured cells. *J Ocul Pharmacol Ther.* 2003;19:501–515.
2. Crowston JG, Lindsey JD, Aihara M, Weinreb RN. Effect of latanoprost on intraocular pressure in mice lacking the prostaglandin FP receptor. *Invest Ophthalmol Vis Sci.* 2004;45:3555–3559.
3. Woodward DF, Krauss AH, Chen J, et al. The pharmacology of bimatoprost (Lumigan). *Surv Ophthalmol.* 2001;45:S337–S345.
4. Resul B, Stjernschantz J, Selen G, Bito L. Structure-activity relationships and receptor profiles of some ocular hypotensive prostanoids. *Surv Ophthalmol.* 1997;41:S47–S52.
5. Sharif NA, Crider JY, Husain S, Kaddour-Djebbar I, Ansari HR, Abdel-Latif AA. Human ciliary muscle cell responses to FP-class prostaglandin analogs: phosphoinositide hydrolysis, intracellular Ca2+ mobilization and MAP kinase activation. *J Ocul Pharmacol Ther.* 2003;19:437–455.
6. Sharif NA, Davis TL, Williams GW. [3H]AL-5848 ([3H]9beta-(+)-Fluprostenol). Carboxylic acid of travoprost (AL-6221), a novel FP prostaglandin to study the pharmacology and autoradiographic localization of the FP receptor. *J Pharm Pharmacol.* 1999;51:685–694.
7. Sharif NA, Kelly CR, Crider JY. Agonist activity of bimatoprost, travoprost, latanoprost, unoprostone isopropyl ester and other prostaglandin analogs at the cloned human ciliary body FP prostaglandin receptor. *J Ocul Pharmacol Ther.* 2002;18:313–324.
8. Sharif NA, Kelly CR, Crider JY. Human trabecular meshwork cell responses induced by bimatoprost, travoprost, unoprostone, and other FP prostaglandin receptor agonist analogues. *Invest Ophthalmol Vis Sci.* 2003;44:715–721.
9. Sharif NA, Kelly CR, Williams GW. Bimatoprost (Lumigan) is an agonist at the cloned human ocular FP prostaglandin receptor: real-time FLIPR-based intracellular Ca(2+) mobilization studies. *Prostaglandins Leukot Essent Fatty Acids.* 2003;68:27–33.
10. Sharif NA, Williams GW, Kelly CR. Bimatoprost and its free acid are prostaglandin FP receptor agonists. *Eur J Pharmacol.* 2001;432:211–221.
11. Stjernschantz JW. From PGF(2alpha)-isopropyl ester to latanoprost: a review of the development of xalatan: the Proctor Lecture. *Invest Ophthalmol Vis Sci.* 2001;42:1134–1145.
12. Camras CB, Toris CB, Sjoquist B, et al. Detection of the free acid of bimatoprost in aqueous humor samples from human eyes treated with bimatoprost before cataract surgery. *Ophthalmology.* 2004;111:2193–2198.
13. Kashiwagi K, Iizuka Y, Tsukahara S. Metabolites of isopropyl unoprostone as potential ophthalmic solutions to reduce intraocular pressure in pigmented rabbits. *Jpn J Pharmacol.* 1999;81:56–62.
14. Kashiwagi K, Kanai N, Tsuchida T, et al. Comparison between isopropyl unoprostone and latanoprost by prostaglandin E(2)induction, affinity to prostaglandin transporter, and intraocular metabolism. *Exp Eye Res.* 2002;74:41–49.
15. Thieme H, Stumpff F, Ottlecz A, Percicot CL, Lambrou GN, Wiederholt M. Mechanisms of action of unoprostone on trabecular meshwork contractility. *Invest Ophthalmol Vis Sci.* 2001;42:3193–3201.
16. Oshika T, Araie M, Sugiyama T, Nakajima M, Azuma I. Effect of bunazosin hydrochloride on intraocular pressure and aqueous humor dynamics in normotensive human eyes. *Arch Ophthalmol.* 1991;109:1569–1574.
17. Zhan GL, Toris CB, Camras CB, Wang YL, Yablonski ME. Bunazosin reduces intraocular pressure in rabbits by increasing uveoscleral outflow. *J Ocul Pharmacol Ther.* 1998;14:217–228.
18. Sugimoto Y, Yamasaki A, Segi E, et al. Failure of parturition in mice lacking the prostaglandin F receptor. *Science.* 1997;277:681–683.
19. Camras CB. Comparison of latanoprost and timolol in patients with ocular hypertension and glaucoma: a six-month masked, multicenter trial in the United States. The United States Latanoprost Study Group. *Ophthalmology.* 1996;103:138–147.
20. Aihara M, Lindsey JD, Weinreb RN. Reduction of intraocular pressure in mouse eyes treated by latanoprost. *Invest Ophthalmol Vis Sci.* 2002;43:146–150.
21. Ota T, Murata H, Sugimoto E, Aihara M, Araie M. Prostaglandin analogues and mouse intraocular pressure: effects of tafluprost, latanoprost, travoprost, and unoprostone, considering 24-hour variation. *Invest Ophthalmol Vis Sci.* 2005;46:2006–2011.
22. Lindsey JD, Kashiwagi K, Boyle D, Kashiwagi F, Firestein GS, Weinreb RN. Prostaglandins increase proMMP-1 and proMMP-3 secretion by human ciliary smooth muscle cells. *Curr Eye Res.* 1996;15:869–875.
23. Lindsey JD, Kashiwagi K, Kashiwagi F, Weinreb RN. Prostaglandin action on ciliary smooth muscle extracellular matrix metabolism: implications for uveoscleral outflow. *Surv Ophthalmol.* 1997;41:S53–S59.
24. Brubaker RF, Schoff EO, Nau CB, Carpenter SP, Chen K, Vandenburgh AM. Effects of AGN 192024, a new ocular hypotensive agent, on aqueous dynamics. *Am J Ophthalmol.* 2001;131:19–24.
25. Richter M, Krauss AH, Woodward DF, Lutjen-Drecoll E. Morphological changes in the anterior eye segment after long-term treatment with different receptor selective prostaglandin agonists and a prostamide. *Invest Ophthalmol Vis Sci.* 2003;44:4419–4426.
26. Noecker RS, Dirks MS, Choplin NT, Bernstein P, Batoosingh AL, Whitcup SM. A six-month randomized clinical trial comparing the intraocular pressure-lowering efficacy of bimatoprost and latanoprost in patients with ocular hypertension or glaucoma. *Am J Ophthalmol.* 2003;135:55–63.
27. Choplin N, Bernstein P, Batoosingh AL, Whitcup SM. A randomized, investigator-masked comparison of diurnal responder rates with bimatoprost and latanoprost in the lowering of intraocular pressure. *Surv Ophthalmol.* 2004;49(suppl 1):S19–S25.
28. DuBiner H, Cooke D, Dirks M, Stewart WC, VanDenburgh AM, Felix C. Efficacy and safety of bimatoprost in patients with elevated intraocular pressure: a 30-day comparison with latanoprost. *Surv Ophthalmol.* 2001;45(suppl 4):S353–S360.
29. Walters TR, DuBiner HB, Carpenter SP, Khan B, VanDenburgh AM. 24-Hour IOP control with once-daily bimatoprost, timolol gel-forming solution, or latanoprost: a 1-month, randomized, comparative clinical trial. *Surv Ophthalmol.* 2004;49(suppl 1):S26–S35.

Prostaglandin Analogues and Mouse Intraocular Pressure: Effects of Tafluprost, Latanoprost, Travoprost, and Unoprostone, Considering 24-Hour Variation

Takashi Ota,[1] *Hiroshi Murata,*[1,2] *Ei-ichiro Sugimoto,*[1,3] *Makoto Aihara,*[1] *and Makoto Araie*[1]

Purpose. To establish a mouse model for the pharmacological analysis of antiglaucoma drugs, considering the effect of variations in IOP during 24 hours on the drugs' effects, and to evaluate the effect of a newly developed FP agonist, tafluprost, on mouse IOP, in comparison with three clinically available prostaglandin (PG) analogues.

Methods. Inbred adult ddY mice were bred and acclimatized under a 12-hour light–dark cycle. With mice under general anesthesia, a microneedle method was used to measure IOP. A single drop of 3 μL of either drug or vehicle solution was topically applied once into one eye in each mouse, in a blinded manner, with the contralateral, untreated eye serving as the control. IOP reduction was evaluated by the difference in IOP between the treated and untreated eyes in the same mouse. First, to determine the period feasible for demonstrating a larger magnitude of ocular hypotensive effect, the 24-hour diurnal variation in mouse IOP was measured, and 0.005% latanoprost was applied at the peak or trough time of variation in 24-hour IOP. The time point of the most hypotensive effect was selected for further studies, to evaluate the effects of PG analogues. Second, mice received tafluprost (0.0003%, 0.0015%, 0.005%, or 0.015%), latanoprost (0.001%, 0.0025%, or 0.005%), travoprost (0.001%, 0.002%, or 0.004%), or isopropyl unoprostone (0.03%, 0.06%, or 0.12%), and each corresponding vehicle solution. IOP was then measured at 1, 2, 3, 6, 9, and 12 hours after drug administration. The ocular hypotensive effects of the other three PG analogues were compared with that of tafluprost. All experiments were conducted in a masked study design.

Results. The IOP in the untreated mouse eye was higher at night than during the day. Latanoprost significantly lowered IOP at night (21.4%), compared with the IOP in the untreated contralateral eye 2 hours after administration. The maximum IOP reduction was 20.2% ± 2.0%, 18.7% ± 2.5%, and 11.2% ± 1.8% of that in the untreated eye 2 hours after administration of 0.005% tafluprost, 0.005% latanoprost, and 0.12% isopropyl unoprostone, respectively, whereas it was 20.8% ± 4.6% at 6 hours with 0.004% travoprost (n = 7~17). The order of ocular hypotensive effects of three clinically used PG analogues in mice was comparable to that in humans. Area under the curve (AUC) analysis revealed dose-dependent IOP reductions for each PG analogue. Tafluprost 0.005% decreased IOP more than 0.005% latanoprost at 3, 6, and 9 hours (P = 0.001–0.027) or 0.12% unoprostone at 2, 3, and 6 hours (P = 0.0004–0.01).

Conclusions. The 24-hour variation in mouse eyes should be taken into consideration when evaluating the reduction of IOP. The mouse model was found to be useful in evaluating the pharmacological response to PG analogues. A newly developed FP agonist, 0.005% tafluprost, lowered normal mouse IOP more effectively than did 0.005% latanoprost. (*Invest Ophthalmol Vis Sci.* 2005;46:2006–2011) DOI:10.1167/iovs.04-1527

Prostaglandin (PG) analogues have been widely used for the treatment of glaucoma and ocular hypertension, because they are more effective in lowering intraocular pressure (IOP) and have considerably fewer systemic side effects than do β-blockers. Currently, four different types of PG analogues—isopropyl unoprostone, latanoprost, travoprost, and bimatoprost—are used for the treatment of glaucoma. Recently, a new PG-analogue, tafluprost (AFP-168), has been developed.[1,2] The intraocular metabolites of these PG analogues, with the exception of unoprostone, show a high affinity for the prostanoid FP receptor (FP).[1–7] FP is expressed in human ocular tissues such as the ciliary body and the sclera.[8,9] Latanoprost and travoprost, both selective FP agonists, have been thought to bind to FP, leading to IOP reduction by causing an increase in uveoscleral outflow.[10] The molecular mechanisms of the ocular hypotensive effects of bimatoprost or unoprostone, however, have not been fully clarified.

The availability of various transgenic mice allows us to investigate the role of a molecule in vivo. To clarify physiological mechanisms in finely structured tissues such as those involved in IOP reduction, in vivo assessment using an animal model is indispensable. The ocular hypotensive effects of latanoprost and aqueous dynamics in mice have recently been demonstrated.[11,12] Latanoprost decreases IOP in a dose-dependent manner,[11] a finding that is supported by the fact that aqueous outflow in mice mainly depends on the uveoscleral outflow pathway.[12] These results suggest the possibility of using prostanoid-receptor knockout mice to investigate the relationship between prostanoid receptors and the reduction of IOP. In fact, Crowston et al.[13] recently found that the latanoprost-induced ocular hypotensive effect is mainly dependent on the FP receptor, since its effect diminishes in FP receptor knockout mice. However, the ocular hypotensive effects of PG analogues other than latanoprost have not been fully investigated in mouse eyes, and the influence of the 24-hour variation in IOP on ocular hypotensive effects has not yet been considered.

Thus, the present investigation was undertaken to establish a ddY mouse model for the pharmacological analysis of antiglaucoma drugs, taking the 24-hour IOP variation into consid-

From the [1]Department of Ophthalmology, University of Tokyo School of Medicine, Tokyo, Japan; the [2]Tokyo Metropolitan Geriatric Medical Center, Tokyo, Japan; and the [3]Department of Ophthalmology, University of Hiroshima School of Medicine, Hiroshima, Japan.

Supported by Grant-in-Aid for Science Research (A)14207049 from the Japanese Ministry of Education, Culture, Sports, Science, and Technology (MAr).

Submitted for publication December 28, 2004; revised February 12, 2005; accepted February 14, 2005.

Disclosure: **T. Ota**, None; **H. Murata**, None; **E. Sugimoto**, None; **M. Aihara**, None; **M. Araie**, None

The publication costs of this article were defrayed in part by page charge payment. This article must therefore be marked "*advertisement*" in accordance with 18 U.S.C. §1734 solely to indicate this fact.

Corresponding author: Makoto Aihara, Department of Ophthalmology, University of Tokyo School of Medicine, 7-3-1 Hongo Bunkyo-ku, Tokyo 113-8655, Japan; aihara-tky@umin.ac.jp.

Investigative Ophthalmology & Visual Science, June 2005, Vol. 46, No. 6